Eur. Phys. J. C 51, 249–269 (2007)
DOI 10.1140/epjc/s10052-007-0304-9

THE EUROPEAN PHYSICAL JOURNAL C

Regular Article – Experimental Physics

Investigation of Colour Reconnection in WW events with the DELPHI detector at LEP-2

The DELPHI Collaboration

J. Abdallah[26], P. Abreu[23], W. Adam[55], P. Adzic[12], T. Albrecht[18], R. Alemany-Fernandez[9], T. Allmendinger[18], P.P. Allport[24], U. Amaldi[30], N. Amapane[48], S. Amato[52], E. Anashkin[37], A. Andreazza[29], S. Andringa[23], N. Anjos[23], P. Antilogus[26], W-D. Apel[18], Y. Arnoud[15], S. Ask[27], B. Asman[47], J.E. Augustin[26], A. Augustinus[9], P. Baillon[9], A. Ballestrero[49], P. Bambade[21], R. Barbier[28], D. Bardin[17], G.J. Barker[57], A. Baroncelli[40], M. Battaglia[9], M. Baubillier[26], K-H. Becks[58], M. Begalli[7], A. Behrmann[58], E. Ben-Haim[21], N. Benekos[33], A. Benvenuti[5], C. Berat[15], M. Berggren[26], L. Berntzon[47], D. Bertrand[2], M. Besancon[41], N. Besson[41], D. Bloch[10], M. Blom[32], M. Bluj[56], M. Bonesini[30], M. Boonekamp[41], P.S.L. Booth[24,a], G. Borisov[22], O. Botner[53], B. Bouquet[21], T.J.V. Bowcock[24], I. Boyko[17], M. Bracko[44], R. Brenner[53], E. Brodet[36], P. Bruckman[19], J.M. Brunet[8], B. Buschbeck[55], P. Buschmann[58], M. Calvi[30], T. Camporesi[9], V. Canale[39], F. Carena[9], N. Castro[23], F. Cavallo[5], M. Chapkin[43], Ph. Charpentier[9], P. Checchia[37], R. Chierici[9], P. Chliapnikov[43], J. Chudoba[9], S.U. Chung[9], K. Cieslik[19], P. Collins[9], R. Contri[14], G. Cosme[21], F. Cossutti[50], M.J. Costa[54], D. Crennell[38], J. Cuevas[35], J. D'Hondt[2], J. Dalmau[47], T. da Silva[52], W. Da Silva[26], G. Della Ricca[50], A. De Angelis[51], W. De Boer[18], C. De Clercq[2], B. De Lotto[51], N. De Maria[48], A. De Min[37], L. de Paula[52], L. Di Ciaccio[39], A. Di Simone[40], K. Doroba[56], J. Drees[58,9], G. Eigen[4], T. Ekelof[53], M. Ellert[53], M. Elsing[9], M.C. Espirito Santo[23], G. Fanourakis[12], D. Fassouliotis[12,3], M. Feindt[18], J. Fernandez[42], A. Ferrer[54], F. Ferro[14], U. Flagmeyer[58], H. Foeth[9], E. Fokitis[33], F. Fulda-Quenzer[21], J. Fuster[54], M. Gandelman[52], C. Garcia[54], Ph. Gavillet[9], E. Gazis[33], R. Gokieli[9,56], B. Golob[44,46], G. Gomez-Ceballos[42], P. Goncalves[23], E. Graziani[40], G. Grosdidier[21], K. Grzelak[56], J. Guy[38], C. Haag[18], A. Hallgren[53], K. Hamacher[58], K. Hamilton[36], S. Haug[34], F. Hauler[18], V. Hedberg[27], M. Hennecke[18], H. Herr[9,a], J. Hoffman[56], S-O. Holmgren[47], P.J. Holt[9], M.A. Houlden[24], J.N. Jackson[24], G. Jarlskog[27], P. Jarry[41], D. Jeans[36], E.K. Johansson[47], P.D. Johansson[47], P. Jonsson[28], C. Joram[9], L. Jungermann[18], F. Kapusta[26], S. Katsanevas[28], E. Katsoufis[33], G. Kernel[44], B.P. Kersevan[44,46], U. Kerzel[18], B.T. King[24], N.J. Kjaer[9], P. Kluit[32], P. Kokkinias[12], C. Kourkoumelis[3], O. Kouznetsov[17], Z. Krumstein[17], M. Kucharczyk[19], J. Lamsa[1], G. Leder[55], F. Ledroit[15], L. Leinonen[47], R. Leitner[31], J. Lemonne[2], V. Lepeltier[21], T. Lesiak[19], W. Liebig[58], D. Liko[55], A. Lipniacka[47], J.H. Lopes[52], J.M. Lopez[35], D. Loukas[12], P. Lutz[41], L. Lyons[36], J. MacNaughton[55], A. Malek[58], S. Maltezos[33], F. Mandl[55], J. Marco[42], R. Marco[42], B. Marechal[52], M. Margoni[37], J-C. Marin[9], C. Mariotti[9], A. Markou[12], C. Martinez-Rivero[42], J. Masik[13], N. Mastroyiannopoulos[12], F. Matorras[42], C. Matteuzzi[30], F. Mazzucato[37], M. Mazzucato[37], R. Mc Nulty[24], C. Meroni[29], E. Migliore[48], W. Mitaroff[55], U. Mjoernmark[27], T. Moa[47], M. Moch[18], K. Moenig[9,11], R. Monge[14], J. Montenegro[32], D. Moraes[52], S. Moreno[23], P. Morettini[14], U. Mueller[58], K. Muenich[58], M. Mulders[32], L. Mundim[7], W. Murray[38], B. Muryn[20], G. Myatt[36], T. Myklebust[34], M. Nassiakou[12], F. Navarria[5], K. Nawrocki[56], R. Nicolaidou[41], M. Nikolenko[17,10], A. Oblakowska-Mucha[20], V. Obraztsov[43], A. Olshevski[17], A. Onofre[23], R. Orava[16], K. Osterberg[16], A. Ouraou[41], A. Oyanguren[54], M. Paganoni[30], S. Paiano[5], J.P. Palacios[24], H. Palka[19], Th.D. Papadopoulou[33], L. Pape[9], C. Parkes[25], F. Parodi[14], U. Parzefall[9], A. Passeri[40], O. Passon[58], L. Peralta[23], V. Perepelitsa[54], A. Perrotta[5], A. Petrolini[14], J. Piedra[42], L. Pieri[40], F. Pierre[41], M. Pimenta[23], E. Piotto[9], T. Podobnik[44,46], V. Poireau[9], M.E. Pol[6], G. Polok[19], V. Pozdniakov[17], N. Pukhaeva[17], A. Pullia[30], J. Rames[13], A. Read[34], P. Rebecchi[9], J. Rehn[18], D. Reid[32], R. Reinhardt[58], P. Renton[36], F. Richard[21], J. Ridky[13], M. Rivero[42], D. Rodriguez[42], A. Romero[48], P. Ronchese[37], P. Roudeau[21], T. Rovelli[5], V. Ruhlmann-Kleider[41], D. Ryabtchikov[43], A. Sadovsky[17], L. Salmi[16], J. Salt[54], C. Sander[18], A. Savoy-Navarro[26], U. Schwickerath[9], R. Sekulin[38], M. Siebel[58], A. Sisakian[17], G. Smadja[28], O. Smirnova[27], A. Sokolov[43], A. Sopczak[22], R. Sosnowski[56], T. Spassov[9], M. Stanitzki[18], A. Stocchi[21], J. Strauss[55], B. Stugu[4], M. Szczekowski[56], M. Szeptycka[56], T. Szumlak[20], T. Tabarelli[30], A.C. Taffard[24], F. Tegenfeldt[53], J. Timmermans[32,b], L. Tkatchev[17], M. Tobin[24], S. Todorovova[13], B. Tome[23], A. Tonazzo[30], P. Tortosa[54], P. Travnicek[13], D. Treille[9], G. Tristram[8], M. Trochimczuk[56], C. Troncon[29], M-L. Turluer[41], I.A. Tyapkin[17], P. Tyapkin[17], S. Tzamarias[12], V. Uvarov[43], G. Valenti[5], P. Van Dam[32], J. Van Eldik[9], N. van Remortel[16], I. Van Vulpen[9], G. Vegni[29], F. Veloso[23], W. Venus[38], P. Verdier[28], V. Verzi[39], D. Vilanova[41], L. Vitale[50], V. Vrba[13], H. Wahlen[58], A.J. Washbrook[24], C. Weiser[18], D. Wicke[9], J. Wickens[2], G. Wilkinson[36], M. Winter[10], M. Witek[19], O. Yushchenko[43], A. Zalewska[19], P. Zalewski[56], D. Zavrtanik[45], V. Zhuravlov[17], N.I. Zimin[17], A. Zintchenko[17], M. Zupan[12]

[1] Department of Physics and Astronomy, Iowa State University, Ames IA 50011-3160, USA
[2] IIHE, ULB-VUB, Pleinlaan 2, 1050 Brussels, Belgium
[3] Physics Laboratory, University of Athens, Solonos Str. 104, 10680 Athens, Greece
[4] Department of Physics, University of Bergen, Allégaten 55, 5007 Bergen, Norway
[5] Dipartimento di Fisica, Università di Bologna and INFN, Via Irnerio 46, 40126 Bologna, Italy
[6] Centro Brasileiro de Pesquisas Físicas, rua Xavier Sigaud 150, 22290 Rio de Janeiro, Brazil
[7] Inst. de Física, Univ. Estadual do Rio de Janeiro, rua São Francisco Xavier 524, Rio de Janeiro, Brazil
[8] Collège de France, Lab. de Physique Corpusculaire, IN2P3-CNRS, 75231 Paris Cedex 05, France
[9] CERN, 1211 Geneva 23, Switzerland
[10] Institut de Recherches Subatomiques, IN2P3 - CNRS/ULP - BP20, 67037 Strasbourg Cedex, France
[11] Now at DESY-Zeuthen, Platanenallee 6, 15735 Zeuthen, Germany
[12] Institute of Nuclear Physics, N.C.S.R. Demokritos, P.O. Box 60228, 15310 Athens, Greece
[13] FZU, Inst. of Phys. of the C.A.S. High Energy Physics Division, Na Slovance 2, 180 40, Praha 8, Czech Republic
[14] Dipartimento di Fisica, Università di Genova and INFN, Via Dodecaneso 33, 16146 Genova, Italy
[15] Institut des Sciences Nucléaires, IN2P3-CNRS, Université de Grenoble 1, 38026 Grenoble Cedex, France
[16] Helsinki Institute of Physics and Department of Physical Sciences, P.O. Box 64, 00014 University of Helsinki, Finland
[17] Joint Institute for Nuclear Research, Dubna, Head Post Office, P.O. Box 79, 101 000 Moscow, Russian Federation
[18] Institut für Experimentelle Kernphysik, Universität Karlsruhe, Postfach 6980, 76128 Karlsruhe, Germany
[19] Institute of Nuclear Physics PAN, Ul. Radzikowskiego 152, 31142 Krakow, Poland
[20] Faculty of Physics and Nuclear Techniques, University of Mining and Metallurgy, 30055 Krakow, Poland
[21] Université de Paris-Sud, Lab. de l'Accélérateur Linéaire, IN2P3-CNRS, Bât. 200, 91405 Orsay Cedex, France
[22] School of Physics and Chemistry, University of Lancaster, Lancaster LA1 4YB, UK
[23] LIP, IST, FCUL – Av. Elias Garcia, 14-1^{o}, 1000 Lisboa Codex, Portugal
[24] Department of Physics, University of Liverpool, P.O. Box 147, Liverpool L69 3BX, UK
[25] Dept. of Physics and Astronomy, Kelvin Building, University of Glasgow, Glasgow G12 8QQ, UK
[26] LPNHE, IN2P3-CNRS, Univ. Paris VI et VII, Tour 33 (RdC), 4 place Jussieu, 75252 Paris Cedex 05, France
[27] Department of Physics, University of Lund, Sölvegatan 14, 223 63 Lund, Sweden
[28] Université Claude Bernard de Lyon, IPNL, IN2P3-CNRS, 69622 Villeurbanne Cedex, France
[29] Dipartimento di Fisica, Università di Milano and INFN-MILANO, Via Celoria 16, 20133 Milan, Italy
[30] Dipartimento di Fisica, Univ. di Milano-Bicocca and INFN-MILANO, Piazza della Scienza 3, 20126 Milan, Italy
[31] IPNP of MFF, Charles Univ., Areal MFF, V Holesovickach 2, 180 00, Praha 8, Czech Republic
[32] NIKHEF, Postbus 41882, 1009 DB Amsterdam, The Netherlands
[33] National Technical University, Physics Department, Zografou Campus, 15773 Athens, Greece
[34] Physics Department, University of Oslo, Blindern, 0316 Oslo, Norway
[35] Dpto. Fisica, Univ. Oviedo, Avda. Calvo Sotelo s/n, 33007 Oviedo, Spain
[36] Department of Physics, University of Oxford, Keble Road, Oxford OX1 3RH, UK
[37] Dipartimento di Fisica, Università di Padova and INFN, Via Marzolo 8, 35131 Padua, Italy
[38] Rutherford Appleton Laboratory, Chilton, Didcot OX11 OQX, UK
[39] Dipartimento di Fisica, Università di Roma II and INFN, Tor Vergata, 00173 Rome, Italy
[40] Dipartimento di Fisica, Università di Roma III and INFN, Via della Vasca Navale 84, 00146 Rome, Italy
[41] DAPNIA/Service de Physique des Particules, CEA-Saclay, 91191 Gif-sur-Yvette Cedex, France
[42] Instituto de Fisica de Cantabria (CSIC-UC), Avda. los Castros s/n, 39006 Santander, Spain
[43] Inst. for High Energy Physics, Serpukov P.O. Box 35, Protvino, (Moscow Region), Russian Federation
[44] J. Stefan Institute, Jamova 39, 1000 Ljubljana, Slovenia
[45] Laboratory for Astroparticle Physics, University of Nova Gorica, Kostanjeviska 16a, 5000 Nova Gorica, Slovenia
[46] Department of Physics, University of Ljubljana, 1000 Ljubljana, Slovenia
[47] Fysikum, Stockholm University, Box 6730, 113 85 Stockholm, Sweden
[48] Dipartimento di Fisica Sperimentale, Università di Torino and INFN, Via P. Giuria 1, 10125 Turin, Italy
[49] INFN, Sezione di Torino and Dipartimento di Fisica Teorica, Università di Torino, Via Giuria 1, 10125 Turin, Italy
[50] Dipartimento di Fisica, Università di Trieste and INFN, Via A. Valerio 2, 34127 Trieste, Italy
[51] Istituto di Fisica, Università di Udine and INFN, 33100 Udine, Italy
[52] Univ. Federal do Rio de Janeiro, C.P. 68528 Cidade Univ., Ilha do Fundão 21945-970 Rio de Janeiro, Brazil
[53] Department of Radiation Sciences, University of Uppsala, P.O. Box 535, 751 21 Uppsala, Sweden
[54] IFIC, Valencia-CSIC, and D.F.A.M.N., U. de Valencia, Avda. Dr. Moliner 50, 46100 Burjassot (Valencia), Spain
[55] Institut für Hochenergiephysik, Österr. Akad. d. Wissensch., Nikolsdorfergasse 18, 1050 Vienna, Austria
[56] Inst. Nuclear Studies and University of Warsaw, Ul. Hoza 69, 00681 Warsaw, Poland
[57] Now at University of Warwick, Coventry CV4 7AL, UK
[58] Fachbereich Physik, University of Wuppertal, Postfach 100 127, 42097 Wuppertal, Germany

Received: 13 December 2006 / Revised version: 23 March 2007 /
Published online: 5 May 2007 –

Abstract. In the reaction $e^+e^- \to WW \to (q_1\bar{q}_2)(q_3\bar{q}_4)$ the usual hadronization models treat the colour singlets $q_1\bar{q}_2$ and $q_3\bar{q}_4$ coming from two W bosons independently. However, since the final state partons may coexist in space and time, cross-talk between the two evolving hadronic systems may be possible during fragmentation through soft gluon exchange. This effect is known as colour reconnection. In this article the results of the investigation of colour reconnection effects in fully hadronic decays of W pairs in DELPHI at LEP are presented. Two complementary analyses were performed, studying the particle flow between jets and W mass estimators, with negligible correlation between them, and the results were combined and compared to models. In the framework of the SK-I model, the value for its κ parameter most compatible with the data was found to be:

$$\kappa_{\text{SK-I}} = 2.2^{+2.5}_{-1.3}$$

corresponding to the probability of reconnection $\mathcal{P}_{\text{reco}}$ to be in the range $0.31 < \mathcal{P}_{\text{reco}} < 0.68$ at 68% confidence level with its best value at 0.52.

1 Introduction

The space-time development of a hadronic system is still poorly understood, and models are necessary to transform a partonic system, governed by perturbative QCD, to final state hadrons observed in the detectors.

WW events produced in e^+e^- collisions at LEP-2 constitute a unique laboratory to study and test the evolution of such hadronic systems, because of the clean environment and the well-defined initial energy in the process. Of particular interest is the possibility to study separately one single evolving hadronic system (one of the W bosons decaying semi-leptonically, the other decaying hadronically), and compare it with two hadronic systems evolving at the same time (both W bosons decaying hadronically).

Interconnection effects between the products of the hadronic decays of the two W bosons (in the same event) are expected since the lifetime of the W bosons ($\tau_W \simeq \hbar/\Gamma_W \simeq 0.1\,\text{fm}/c$) is an order of magnitude smaller than the typical hadronization times. These effects can happen at two levels:

– in the evolution of the parton shower, between partons from different hadronic systems by exchanging coloured gluons [1] (this effect is called *Colour Reconnection* (CR) for historical reasons);
– between the final state hadrons, due to quantum-mechanical interference, mainly due to Bose–Einstein correlations (BEC) between identical bosons (e.g. pions with the same charge).

A detailed study by DELPHI of this second effect was recently published [2].

The first effect, the possible presence of colour flow between the two W hadronization systems, is the topic studied in this paper. This effect is worthy of study in its own right and for the possible effects induced on the W mass measurement in fully hadronic events (see for instance [3] for an introduction and [4] for an experimental review).

The effects at the perturbative level are expected to be small [3], whereas they may be large at the hadronization level (many soft gluons sharing the space-time) for which models have to be used to compare with the data.

The most tested model is the Sjöstrand–Khoze "Type 1" CR model SK-I [5]. This model of CR is based on the Lund string fragmentation phenomenology. The strings are considered as colour flux tubes with some volume, and reconnection occurs when these tubes overlap. The probability of reconnection in an event is parameterised by the value κ, set globally by the user, according to the space-time volume overlap of the two strings, V_{overlap}:

$$\mathcal{P}_{\text{reco}}(\kappa) = 1 - \mathrm{e}^{-\kappa V_{\text{overlap}}}\,. \tag{1}$$

The parameter κ was introduced in the SK-I model to allow a variation of the percentage of reconnected events and facilitate studies of sensitivity to the effect. In this model only one string reconnection per event was allowed. The authors of the model propose the value of $\kappa = 0.66$ to give similar amounts of reconnection as other models of Colour Reconnection. By comparing the data with the model predictions evaluated at several κ values, it is possible to determine the value of κ most consistent with the data and extract the corresponding reconnection probability. Another model was proposed by the same authors, considering the colour flux tubes as infinitely thin, which allows for Colour Reconnection in the case the tubes cross each other and provided the total string length is reduced (SK-II′). This last model was not tested.

Two further models are tested here, these are the models implemented in HERWIG [6, 7] and ARIADNE [8, 9] Monte Carlo programs. In HERWIG the partons are reconnected, with a reconnection probability of 1/9, if the reconnection results in a smaller total cluster mass. In ARIADNE, which implements an adapted version of the Gustafson–Häkkinen model [10], the model used [11] allows for reconnections between partons originating in the same W boson, or from different W bosons if they have an energy smaller than the width of the W boson (this model will be referred as "AR-2").

Colour Reconnection has been previously investigated in DELPHI by comparing inclusive distributions of charged particles, such as the charged-particle multiplicity distribution or the production of identified (heavy) particles, in fully hadronic WW events and the distributions in semi-leptonic WW events. The investigations did not show any effect as they were limited by statistical and systematic

[a] deceased
[b] e-mail: Jan.Timmermans@cern.ch

errors and excluded only the most extreme models of CR (see [12, ?]).

This article presents the results of the investigations of colour reconnection effects in hadronically decaying W pairs using two techniques. The first, proposed by L3 in [14], looks at the particle flow between the jets in a 4-jet WW event. The second, proposed by DELPHI in [15], takes into account the different sensitivity to Colour Reconnection of several W mass estimators. The first technique is more independent of the model and it can provide comparisons based on data. The second technique is more dependent on the model tested, but has a much larger sensitivity to the models SK-I and HERWIG. Since the particle flow and W mass estimator methods were found to be largely uncorrelated a combination of the results of these two methods is provided.

The paper is organised as follows. In the next section, the LEP operation and the components of the DELPHI detector relevant to the analyses are briefly described. In Sect. 3 data and simulation samples are explained. Then both of the analysis methods discussed above are described and their results presented in Sects. 4 and 5. The combination of the results is given in Sect. 6 and conclusions are drawn in the seventh and final section.

2 LEP operation and detector description

At LEP-2, the second phase of the e^+e^- collider at CERN, the accelerator was operated at centre-of-mass energies above the threshold for double W boson production from 1996 to 2000. In this period, the DELPHI experiment collected about 12 000 WW events corresponding to a total integrated luminosity of 661 pb^{-1}. About 46% of the WW events are $WW \to q_1\bar{q}_2q_3\bar{q}_4$ events (fully hadronic), and 44% are $WW \to q_1\bar{q}_2\ell\bar{\nu}$, where ℓ is a lepton (semi-leptonic).

The detailed description of the DELPHI detector and its performance is provided in [16, 17]. A brief summary of the main characteristics of the detector important for the analyses follows.

The tracking system of DELPHI consisted of a time projection chamber (TPC), the main tracking device of DELPHI, and was complemented by a vertex detector (VD) closest to the beam pipe, the inner and the outer detectors in the barrel region, and two forward chambers in the end caps. It was embedded in a 1.2 T magnetic field, aligned parallel to the beam axis.

The electromagnetic calorimeter consisted of the high density projection chamber (HPC) in the barrel region, the forward electromagnetic calorimeter (FEMC) and the small angle tile calorimeter (STIC) in the forward regions, complemented by detectors to tag the passage of electron–positron pairs from photons converted in the regions between the FEMC and the HPC. The total depths of the calorimeters corresponded to about 18 radiation lengths. The hadronic calorimeter was composed of instrumented iron with a total depth along the shortest trajectory for a neutral particle of 6 interaction lengths, and covered 98% of the total solid angle. Embedded in the hadronic calorimeter were two planes of muon drift chambers to tag the passage of muons. The whole detector was surrounded by a further double plane of staggered muon drift chambers.

For LEP-2, the DELPHI detector was upgraded as described in the following.

Changes were made to some of the subdetectors, the trigger system [18], the run control and the algorithms used in the offline reconstruction of tracks, which improved the performance compared to the earlier LEP-1 period.

The major changes were the extensions of the vertex detector (VD) and the inner detector (ID), and the inclusion of the very forward tracker (VFT) [19], which increased the coverage of the silicon tracker to polar angles with respect to the z-axis[1] of $11^\circ < \theta < 169^\circ$. To further improve the track reconstruction efficiency in the forward regions of DELPHI, the tracking algorithms and the alignment and calibration procedures were optimised for LEP-2.

Changes were also made to the electronics of the trigger and timing system which improved the stability of the running during data taking. The trigger conditions were optimised for LEP-2 running, to give high efficiency for 2- and 4-fermion processes in the Standard Model and also to give sensitivity to events which may have been signatures of new physics. In addition, improvements were made to the operation of the detector during the LEP operating states, to prepare the detector for data taking at the very start of stable collisions of the e^+e^- beams, and to respond to adverse background from LEP when it arose. These changes led to an overall improvement in the efficiency for collecting the delivered luminosity from about 85% in 1995, before the start of LEP-2, to about 95% at the end in 2000.

During the operation of the DELPHI detector in 2000 one of the 12 sectors of the central tracking chamber, the TPC, failed. After 1st September it was not possible to detect the tracks left by charged particles inside the broken sector. The data affected corresponds to around 1/4 of the data collected in 2000. Nevertheless, the redundancy of the tracking system of DELPHI meant that tracks passing through the sector could still be reconstructed from signals in any of the other tracking detectors. As a result, the track reconstruction efficiency was only slightly reduced in the region covered by the broken sector, but the track parameter resolutions were degraded compared with the data taken prior to the failure of this sector.

3 Data and simulation samples

The analyses presented here use the data collected by DELPHI in the years 1997 to 2000, at centre-of-mass energies $\sqrt{s}$ between 183 and 209 GeV. The data collected in the year 2000 with the TPC working in full, with centre-of-mass energies from 200 to 208 GeV and a integrated lumi-

[1] The DELPHI coordinate system is a right-handed system with the z-axis collinear with the incoming electron beam, and the x-axis pointing to the centre of the LEP accelerator.

nosity weighted average centre-of-mass energy of 206 GeV, were analysed together. Data acquired with the TPC with a broken sector, corresponding to a integrated luminosity weighted average centre-of-mass energy of 207 GeV, were analysed separately and included in the results presented here.

The total integrated luminosity of the data sample is $660.8\,\mathrm{pb}^{-1}$, and the integrated luminosity weighted average centre-of-mass energy of the data is 197.1 GeV.

To compare with the expected results from processes in the Standard Model including or not including CR, Monte Carlo (MC) simulation was used to generate events and simulate the response of the DELPHI detector. These events were reconstructed and analysed with the same programs as used for the real data.

The 4-fermion final states were generated with the code described in [20], based on WPHACT [21, 22], for the WW signal (charged currents) and for the ZZ background (neutral currents), after which the events were fragmented with PYTHIA [23, 24] tuned to DELPHI data [25]. The same WW events generated at 189, 200 and 206 GeV were also fragmented with PYTHIA implementing the SK-I model, with 100% reconnection probability. The systematic effects of fragmentation were studied using the above WW samples and WW samples generated with WPHACT and fragmented with either ARIADNE [8, 9] or HERWIG [6, 7] at 183, 189, 200 and 206 GeV. For systematic studies of Bose–Einstein correlations (BEC), WW samples generated with WPHACT and fragmented with PYTHIA implementing the BE_{32} model [26] of BEC, were used at all energies, except at 207 GeV. The integrated luminosity of the simulated samples was at least 10 times that of the data of the corresponding year, and the majority corresponded to 100 times that of the data.

To test the consistency of the SK-I model and measure the κ parameter, large WW samples were generated in an early stage of this work with EXCALIBUR [27] at 200 and 206 GeV, keeping only the fully hadronic decays. These samples were then fragmented with PYTHIA. It was verified for smaller subsets that the results using these large samples and the samples generated later with WPHACT are compatible.

The $q\bar{q}(\gamma)$ background events were generated at all energies with KK2f [28, 29] and fragmented with PYTHIA. For systematic studies, similar KK2f samples fragmented with ARIADNE [8, 9] were used at 183, 189, 200 and 206 GeV.

These samples will be referred to as "DELPHI samples".

At 189 GeV, to compare with the other LEP experiments and with different CR models, 6 samples generated with KORALW [30] for the 4-fermion final states were also used. These samples [2] will be referred to as "Cetraro samples". The events in the different samples have the final state quarks generated with the same kinematics, and differ only in the parton shower evolution and fragmentation. Three samples were fragmented respectively with PYTHIA, ARIADNE and HERWIG (using the tuning of the ALEPH collaboration), with no CR implementation. Three other samples were fragmented in the same manner but now implementing several CR models: the SK-I model with 100% reconnection probability, the AR-2 model, and the HERWIG implementation of CR with 1/9 of reconnected events, respectively.

[2] produced by ALEPH after the LEP-W Physics Workshop in Cetraro, Italy, October 2001

4 The particle flow method

The first of the two analyses presented in this paper is based on the so-called "particle flow method". The particle flow algorithm is based on the selection of special event topologies, in order to obtain well defined regions between any two jets originating from the same W (called the Inside-W region) or from different W's (called the Between-W region). It is expected that Colour Reconnection decreases (increases) particle production in the Inside-W (Between-W) region. Hence, by studying the particle production in the inter-jet regions it is possible to measure the effects of Colour Reconnection. However, this method requires a selection of events with a suitable topology (see below) which has a low efficiency ($\lesssim 25\%$).

4.1 Event and particle selection

Events with both W's decaying into $q_1\bar{q}_2$ are characterised by high multiplicity, large visible energy, and the tendency of the particles to be grouped in 4 jets. The background is dominated by $q\bar{q}(\gamma)$ events.

Charged particles were required to have momentum p larger than $100\,\mathrm{MeV}/c$ and below 1.5 times the beam energy, a relative error on the momentum measurement $\Delta p/p < 1$, and polar angle θ with respect to the beam axis between 20° and 160°. To remove tracks from secondary interactions, the distance of closest approach of the extrapolated track to the interaction point was required to be less than 4 cm in the plane perpendicular to the beam axis and less than $4/\sin\theta$ cm along the beam axis, and the reconstructed track length was required to be larger than 30 cm.

Clusters in the electromagnetic or hadronic calorimeters with energy larger than 0.5 GeV and polar angle in the interval $10° < \theta < 170°$, not associated to charged particles, were considered as neutral particles.

The events were pre-selected by requiring at least 12 charged particles, with a sum of the modulus of the momentum transverse to the beam axis, of charged and neutral particles, above 20% of the centre-of-mass energy. These cuts reduced the contributions from gamma–gamma processes and beam–gas interactions to a negligible amount. The momentum distribution of the charged particles for the pre-selected events is shown in Fig. 1 and compared to the expected distribution from the simulation. A good agreement between data and simulation is observed.

About half of the $e^+e^- \to q\bar{q}(\gamma)$ events at high-energy are associated with an energetic photon emitted by one of

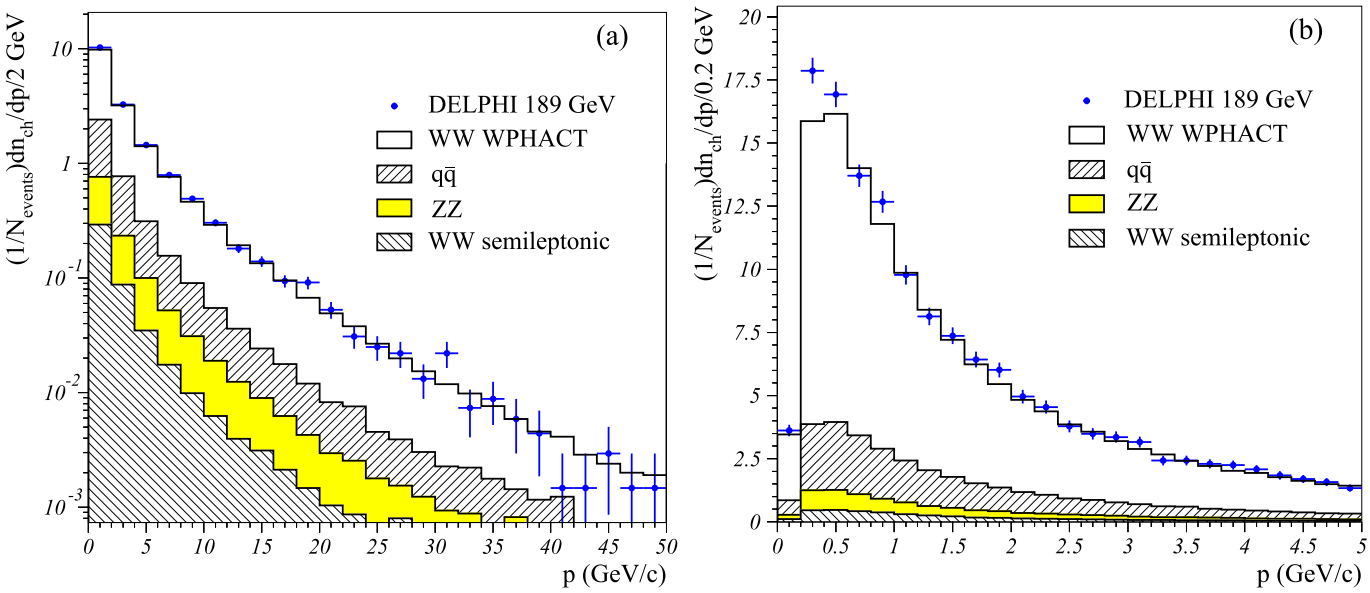

Fig. 1. Momentum distribution for charged particles (range 0–50 GeV/c (**a**) and 0–5 GeV/c (**b**)). *Points* represent the data and the *histograms* represent the contributions from simulation for the different processes (signal (*white*) and background contributions)

the beam electrons or positrons (radiative return events), thus reducing the energy available in the hadronic system to the Z mass. To remove these radiative return events, the effective centre-of-mass energy $\sqrt{s'}$, computed as described in [31], was required to be above 110 GeV. It was verified that this cut does not affect the signal from W pairs, but reduces significantly the contribution from the $q\bar{q}(\gamma)$ process.

In the WW fully hadronic decays four well separated energetic jets are expected which balance the momentum of the event and have a total energy near to the centre-of-mass energy. The charged and neutral particles in the event were thus clustered using the DURHAM algorithm [32], for a separation value of $y_{\rm cut} = 0.005$, and the events were kept if there were 4 and only 4 jets and a multiplicity (charged plus neutral) in each jet larger than 3. The combination of these two cuts removed most of the semi-leptonic WW decays and the 2-jet and 3-jet events of the $q\bar{q}(\gamma)$ background. The charged-particle multiplicity distribution for the selected events at 189 GeV is given in Fig. 2, with data points compared to the histogram from simulation of signal and background processes.

For the study of the charged-particle flow between jets, the initial quark configuration should be well reconstructed with a good quark-jet association. At 183 GeV and above, the produced W bosons are significantly boosted. This produces smaller angles in the laboratory frame of reference between the jets into which the W decays, when compared to these angles at threshold (back-to-back). Hence, this property tends to reduce the ambiguity in the definition of the Between-W and Inside-W regions. The selection criteria were designed in order to minimize the situation of one jet from one W boson appearing in the Inside-W region of the other W boson.

The selection criteria are based on the event topology, with cuts in 4 of the 6 jet–jet angles. The smallest and the second smallest jet–jet angle should be below 100° and not adjacent (not have a common jet). Two other jet–jet angles should be between 100° and 140° and not adjacent (large angles).

In the case that there are two different combinations of jets satisfying the above criteria for the large angles, the combination with the highest sum of large angles is chosen. This selection increases the probability to have a correct pairing of jets to the same W boson.

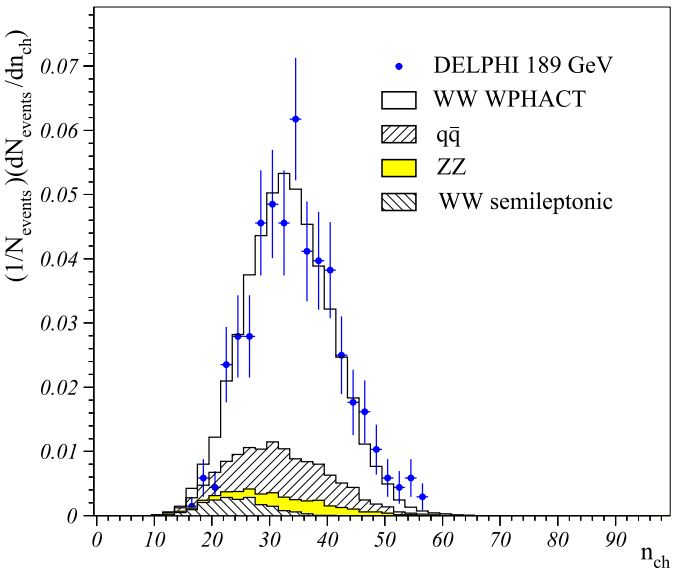

Fig. 2. Uncorrected charged-particle multiplicity distribution at a centre-of-mass energy of 189 GeV. *Points* represent the data and the *histograms* represent the contribution from simulation for the different processes

Table 1. Centre-of-mass energy ($\sqrt{s}$ in GeV), integrated luminosity ($\mathcal{L}$ in pb^{-1}), efficiency and purity of the data samples, number of selected events, number of expected events from 4-jet WW and background processes (total and separated by process), and efficiency of correct pairing of jets to the same W boson

$\sqrt{s}$	$\mathcal{L}$	Eff.	Pur.	$N_{\rm sel}$	MC tot.	WW 4j	$q\bar{q}(\gamma)$	ZZ	W lep.	$\varepsilon_{\rm PAIR}$
183	52.7	22%	74%	127	114.2	84.4	22.3	0.7	7.0	69%
189	157.6	21%	75%	340	341.4	255.9	56.8	2.4	26.4	75%
192	25.9	21%	75%	61	56.1	41.9	9.4	0.4	4.4	77%
196	77.3	19%	74%	176	159.2	117.6	26.2	1.3	14.0	79%
200	83.4	18%	72%	173	165.0	119.5	27.8	1.3	16.4	82%
202	40.6	17%	72%	82	75.7	54.6	12.5	0.7	8.0	82%
206	163.9	15%	70%	282	274.7	193.1	47.8	2.7	31.1	79%
207	59.4	15%	70%	102	99.7	70.1	17.6	1.0	11.1	80%

The integrated luminosity, the efficiency to select 4-jet WW events and the purity of the selected data samples, estimated using simulation, and the number of selected events are summarised for each centre-of-mass energy in Table 1. The numbers of expected events are also given separately for the signal and the background processes, and were estimated using simulation. The efficiency to select the correct pairing of jets to the same W boson, estimated with simulation as the fraction of WW events for which the selected jets 1 and 2 (see later) correspond indeed to the same W boson, is given in the last column of the table.

The efficiency of the event selection criteria decreases with increasing centre-of-mass energy. This is primarily due to the "large" angles being reduced as a result of the increased boost (becoming lower than the cut value of 100°) and "small" angles being increased due to the larger phase-space available (becoming higher than the cut value of 100°). Much for the same reason, the efficiency to assign two jets to the same W boson in the selected events increases slightly with increasing centre-of-mass energy, in opposition to what would happen at threshold with the W boson decaying into two back-to-back jets, that would never be selected to come from the same W boson by the requirement that their interjet angle should be between 100° and 140°.

In the following analysis the jets and planar regions are labeled as shown in Fig. 3: the planar region corresponding to the smallest jet–jet angle is region B in the plane made by jets 2 and 3; the second smallest jet–jet angle corresponds to the planar region D between jets 1 and 4 in the plane made by these two jets; the planar region corresponding to the greatest of the large jet–jet angles in this combination is region A and spans the angle between jets 1 and 2 in the plane made by these jets; and finally region C corresponds to the planar region spanned by the second large angle, between jets 3 and 4 in the plane made by these two jets. In general, the planar regions are not in the same plane, as the decay planes of the W bosons do not coincide, and the large angles in this combination are not necessarily the largest jet–jet angles in the event.

The distribution of the reconstructed masses of the jet pairings (1,2) and (3,4), after applying a 4C kinematic fit requiring energy and momentum conservation, is shown in Fig. 4 (two entries per event). In the figure, data at 189 GeV (points) are compared to the expected distribution from the 4-jet WW signal without CR, plus background processes, estimated using the simulation (histograms). The contribution from the 4-jet WW signal simulation is split between the case in which the two pairs

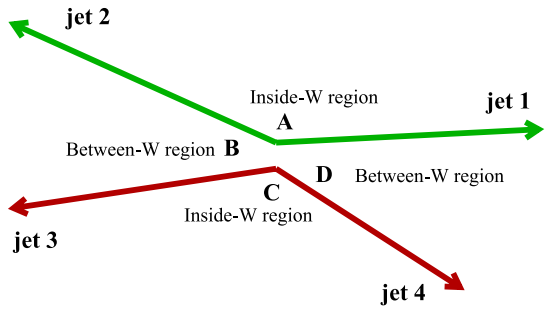

Fig. 3. Schematic drawing of the angular selection

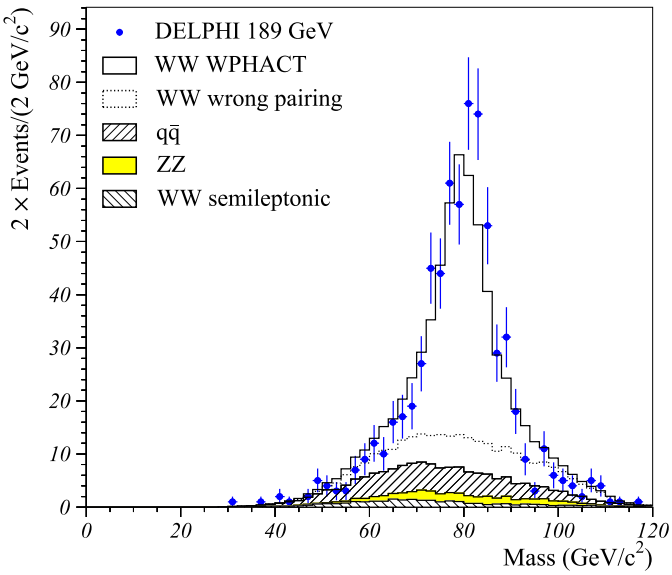

Fig. 4. Reconstructed dijet masses (after a 4C kinematic fit) for the selected pairs at 189 GeV (2 entries per event) (see text)

of jets making the large angles actually come from their parent W bosons and the case in which the jets of a pair come from different W bosons (mismatch).

4.2 Particle flow distribution

The particle flow analysis uses the number of particles in the Inside-W and the Between-W regions. An angular ordering of the jets is performed as in Fig. 3. The two large jet–jet angles in the event are used to define the Inside-W regions, and the two smallest angles span the Between-W regions, the regions between the different W's.

In general, the two W bosons will not decay in the same plane, and this must be accounted for when comparing the particle production in the Inside-W and Between-W regions. So, for each region (A, B, C and D) the particle momenta of all charged particles are projected onto the plane spanned by the jets of that region: jets 1 and 2 for region A; jets 2 and 3 for region B; jets 3 and 4 for region C; jets 4 and 1 for region D. Then, for each particle the rescaled angle Φ_{rescaled} is determined as a ratio of two angles:

$$\Phi_{\mathrm{rescaled}} = \Phi_i / \Phi_r \,, \tag{2}$$

when the particle momentum is projected onto the plane of the region r. The angle Φ_i is then the angle between the projected particle momentum and the first mentioned jet in the definition of the regions given above. The angle Φ_r is the full opening angle between the jets. Hence Φ_{rescaled} varies between 0 and 1 for the particles whose momenta are projected between the pair of jets defining the plane.

However, due to the aplanarity of the event about 9% of the particles in the data and in the 4-jet WW simulation have projected angles outside all four regions. These particles were discarded from further analysis. In the case where a particle could be projected onto more than one region, with $0 < \Phi_{\mathrm{rescaled}} < 1$, the solution with the lower momentum transverse to the region was used. This happened for about 13% of the particles in data, after background subtraction, and in the 4-jet WW simulation.

This leads to the normalised particle flow distribution shown in Fig. 5 at 189 GeV, where the rescaled angle of region A is plotted from 0 to 1, region B from 1 to 2, region C from 2 to 3 and region D from 3 to 4. The statistical error on the bin contents (the average multiplicity per bin of Φ_{rescaled} divided by the bin width) was estimated using the Jackknife method [33], to correctly account for correlations between different bins. In this distribution the regions between the jets coming from the same W bosons (A and C), and from different W bosons (B and D), have the same scale and thus can be easily compared.

After subtracting bin-by-bin the expected background from the observed distributions, we define the Inside-W (Between-W) particle flow as the bin-by-bin sum of regions A and C (B and D). These distributions are compared by performing the bin-by-bin ratio of the Inside-W particle flow to the Between-W particle flow. This ratio of distributions is shown for 189 GeV and 206 GeV in Fig. 6. The

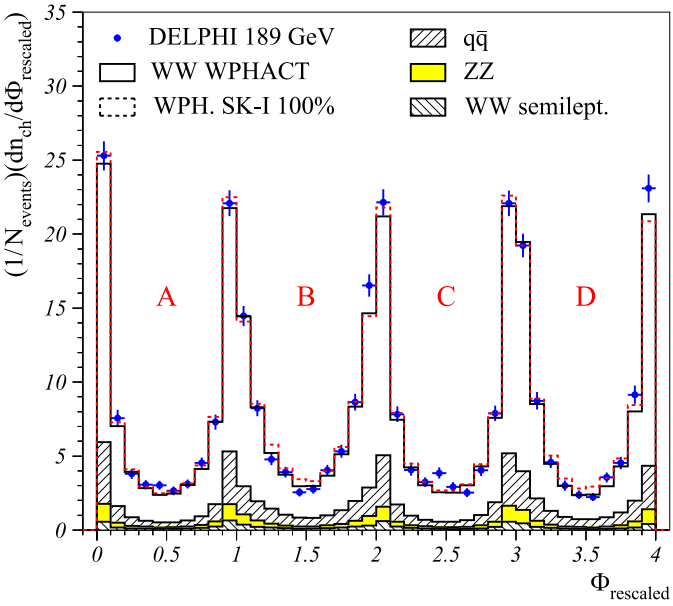

Fig. 5. Normalised charged-particle flow at 189 GeV. The *lines* correspond to the sum of the simulated 4-jet WW signal with the background contributions (estimated from DELPHI MC samples), normalised to the total number of expected events (N_{events}). The *dashed histogram* corresponds to the sum with the simulated 4-jet WW signal generated by WPHACT with 100% SK-I

data points are compared to several fully simulated WW MC samples with and without CR.

A good agreement was found between the predictions using the WPHACT WW MC samples and the predictions based on the KORALW WW MC samples, both for the scenario without CR and for the scenario with CR (SK-I model with 100% probability of reconnection). For both sets of predictions the regions of greatest difference between the two scenarios span the rescaled variable Φ_{rescaled} from 0.2 to 0.8.

4.3 Particle flow ratio

After summing the particle flow distributions for regions A and C, and regions B and D, the resulting distributions are integrated from 0.2 to 0.8. The ratio R of the Inside-W to the Between-W particle flow is then defined as (with Φ being the rescaled variable Φ_{rescaled}):

$$R = \frac{\int_{0.2}^{0.8} \mathrm{d}n_{\mathrm{ch}}/\mathrm{d}\Phi(\mathrm{A}+\mathrm{C})\,\mathrm{d}\Phi}{\int_{0.2}^{0.8} \mathrm{d}n_{\mathrm{ch}}/\mathrm{d}\Phi(\mathrm{B}+\mathrm{D})\,\mathrm{d}\Phi} \,. \tag{3}$$

To take into account possible statistical correlations between particles in the Inside-W and Between-W regions, the statistical error on this ratio R was again estimated through the Jackknife method [33].

The values for R obtained for the different centre-of-mass energies are shown in Table 2, and compared to the expectations from the DELPHI WPHACT WW samples without CR and implementing the SK-I model with 100%

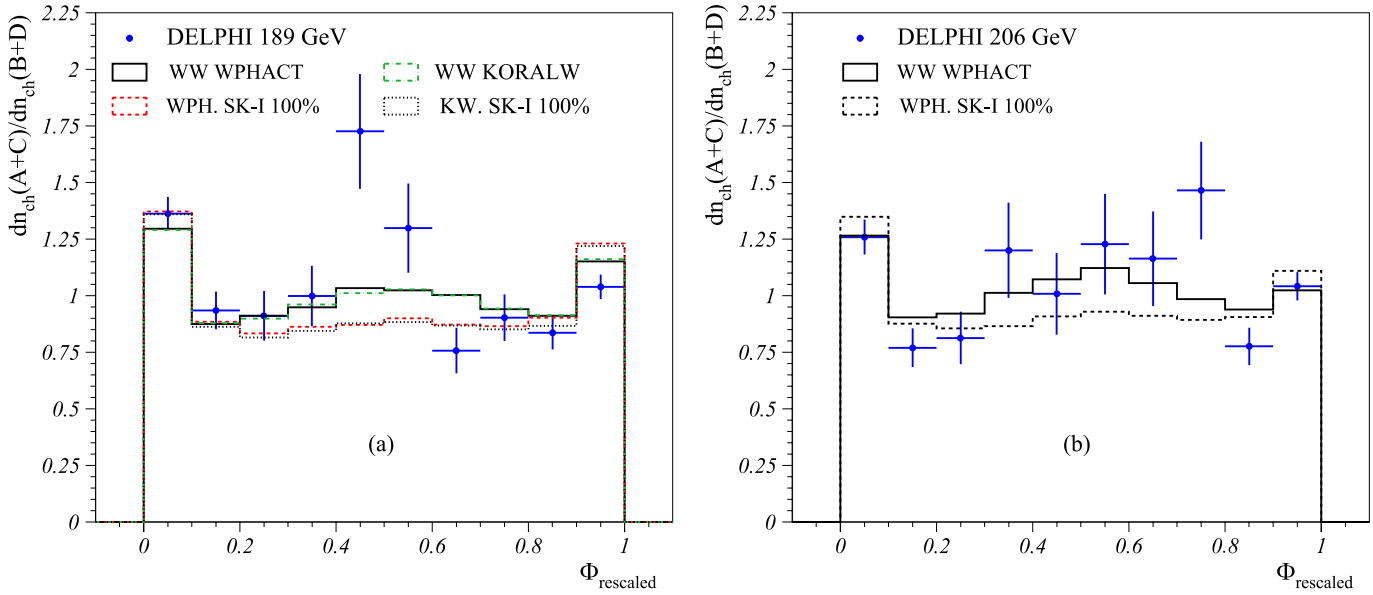

Fig. 6. The ratio of the particle flow distributions $(A+C)/(B+D)$ at 189 GeV (**a**) and at 206 GeV (**b**). The data (*dots*) are compared to WW MC samples generated with WPHACT (DELPHI samples) and KORALW (Cetraro samples), both without CR and implementing the SK-I model with 100% probability of reconnection. The *lines* corresponding to WPHACT are hardly distinguishable from the *lines* corresponding to KORALW in the same condition of implementation of CR

Table 2. Values of the ratio R for each energy (errors are statistical only), and expected values with errors due to limited statistics of the simulation, all from DELPHI WPHACT WW samples

$\sqrt{s}$ (GeV)	R_{Data}	$R_{\text{no CR}}$	$R_{\text{SK-I: 100\%}}$
183	0.889 ± 0.084	0.928 ± 0.005	–
189	1.025 ± 0.063	0.966 ± 0.006	0.864 ± 0.005
192	1.008 ± 0.150	0.970 ± 0.006	–
196	1.041 ± 0.093	0.995 ± 0.006	–
200	0.922 ± 0.084	1.022 ± 0.007	0.889 ± 0.006
202	0.952 ± 0.126	1.015 ± 0.008	–
206	1.116 ± 0.088	1.012 ± 0.008	0.889 ± 0.006
207	1.039 ± 0.135	1.019 ± 0.008	–

reconnection probability. These values for data and MC are plotted as function of the centre-of-mass energy in Fig. 7.

The changes in the value of R for the MC samples are mainly due to the different values of the boost of the W systems. In order to quantify this effect a linear function $R(\sqrt{s}-197.5) = A + B(\sqrt{s}-197.5)$ was fitted to the MC points with CR (with $\sqrt{s}$ in GeV), while for the points without CR the quadratic function $R(\sqrt{s}-197.5) = \alpha + \beta(\sqrt{s}-197.5) + \gamma(\sqrt{s}-197.5)^2$ was assumed (with $\sqrt{s}$ in GeV), giving reasonable χ^2/d.o.f. values. The fits yielded the results shown in Table 3.

The MC without CR shows a stronger dependence on $\sqrt{s}$. The function fitted to this sample was used to rescale the measured values of R for the data collected at different energies to the energy of 189 GeV, the centre-of-mass energy at which the combination of the results of the LEP experiments was proposed in [4]. All the rescaled values were combined with a statistical error-weighted average. The average of the R ratios rescaled to 189 GeV was found to be

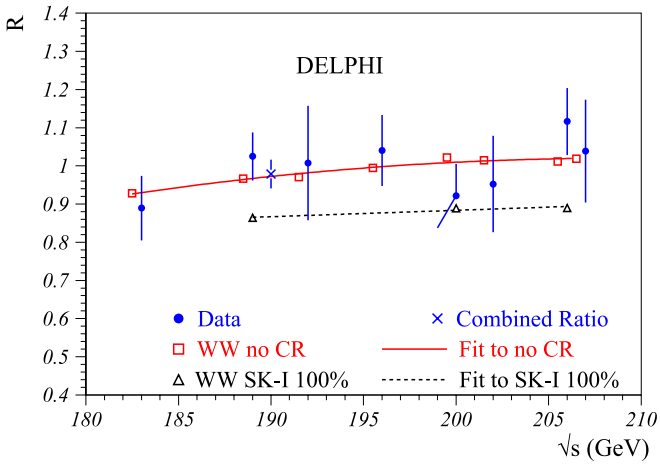

Fig. 7. The ratio R as function of $\sqrt{s}$ for data and MC (DELPHI WPHACT WW samples), and fits to the MC with and without CR, and the combined ratio after rescaling all values to $\sqrt{s} = 189$ GeV (see text). The value of the combined ratio at 189 GeV is shown at a displaced energy (upwards by 1 GeV) for better visibility, as well as all the values for the MC "WW no CR" points and the corresponding fitted curve which are shown at centre-of-mass energies shifted downwards by 0.5 GeV. All errors for the MC values are smaller than the size of the markers

$$\langle R \rangle = 0.979 \pm 0.032\,(\text{stat})\,. \tag{4}$$

Performing the same weighted average when using for the rescaling the fit to the MC with CR, one obtains:

$$\langle R_{\text{CR rescale}} \rangle = 0.987 \pm 0.032\,(\text{stat})\,. \tag{5}$$

Table 3. Results of the fit to the evolution of R with $(\sqrt{s}(\mathrm{GeV}) - 197.5)$

MC Sample	χ^2/DF	α, A	β, B	γ
no CR	7.31/5	1.001 ± 0.003	$(3.20 \pm 0.36) \times 10^{-3}$	$(-1.35 \pm 0.40) \times 10^{-4}$
SK-I 100%	1.46/1	0.880 ± 0.003	$(1.68 \pm 0.44) \times 10^{-3}$	–

Repeating the procedure, but now without rescaling the R ratios, the result is:

$$\langle R_{\text{no rescale}} \rangle = 0.999 \pm 0.033\,(\text{stat})\,. \tag{6}$$

4.4 Study of the systematic errors in the particle flow

The following effects were studied as sources of systematic uncertainties in this analysis.

4.4.1 Fragmentation and detector response

A direct comparison between the particle flow ratios measured in fully hadronic data and MC samples, $R_{4q\,\text{Data}}$ and $R_{4q\,\text{MC}}$, respectively, is hampered by the uncertainties associated with the modelling of the WW fragmentation and the detector response. These systematic uncertainties were estimated using mixed semi-leptonic events. In this technique, two hadronically decaying W bosons from semi-leptonic events were mixed together to emulate a fully hadronic WW decay.

Mixing technique. Semi-leptonic WW decays were selected from the data collected by DELPHI at centre-of-mass energies between 189 and 206 GeV, by requiring two hadronic jets, a well isolated identified muon or electron or, in case of a tau candidate, a well isolated particle, all associated with missing momentum (corresponding to the neutrino) pointing away from the beam pipe. A neural network selection, developed in [34], was used to select the events. The same procedure was applied to the WPHACT samples fragmented with PYTHIA and HERWIG at centre-of-mass energies of 189, 200 and 206 GeV and with ARIADNE at 189 and 206 GeV. The background to this selection was found to be of negligible importance in this analysis. Samples of mixed semi-leptonic events were built separately at each centre-of-mass energy for data and Monte Carlo semi-leptonic samples, following the mixing procedure developed in [2].

In each semi-leptonic event, the lepton (or tau-decay jet) was stripped off and the remaining particles constituted the hadronically decaying W boson. Two hadronically decaying W bosons were then mixed together to emulate a fully hadronic WW decay. The hadronic parts of W bosons were mixed in such a way as to have the parent W bosons back-to-back in the emulated fully hadronic WW decay. To increase the statistics of emulated events, and profiting from the cylindrical symmetry of the detector along the z-axis, the hadronic parts of W bosons were rotated around the z-axis, but were not moved from barrel to forward regions or vice-versa, as detailed in the following.

When mixing the hadronic parts of different W events it was required that the two W's had reconstructed polar angles back-to-back or equal within 10°. In the latter case, when both W's are on the same side of the detector, the z component of the momentum is sign flipped for all the particles in one of the W's.

The particles of one W event were then rotated around the beam axis, in order to have the two W's also back-to-back in the transverse plane. Each semi-leptonic event was used in the mixing procedure between 4 and 9 times, to minimize the statistical error on the particle flow ratio R measured in the mixed semi-leptonic data sample.

The mixed events were then subjected to the same event selection and particle flow analysis used for the fully hadronic events. The particle flow ratios $R_{\text{mixed SL Data}}$ and $R_{\text{mixed SL MC}}$ were measured in the mixed semi-leptonic data and MC samples, respectively, and are plotted as function of the centre-of-mass energy in Fig. 8.

The values of $R_{\text{mixed SL}}$ measured in MC show a dependence on $\sqrt{s}$. This effect is quantified by performing linear fits to the points measured with PYTHIA, ARIADNE and HERWIG, respectively. The differences between the measured slopes were found to be small. The function fitted to the PYTHIA points was used to rescale the values of R measured in data at different energies to 189 GeV. The rescaled values were then combined using as weights the scaled statistical errors. The weighted average R at 189 GeV for the mixed semi-leptonic events built from data was found to be

$$\langle R_{\text{mixed SL Data}} \rangle = 1.052 \pm 0.027\,(\text{stat})\,. \tag{7}$$

For each MC sample, the ratio $R_{\text{mixed SL Data}}/R_{\text{mixed SL MC}}$ was used to calibrate the particle flow ratio measured in the corresponding fully hadronic sample, $R_{4q\,\text{MC}}$, to compare it to the ratio measured in the data, $\langle R_{4q\,\text{Data}} \rangle$. The correction factor $R_{\text{mixed SL Data}}/R_{\text{mixed SL MC}}$ was computed from the values of R rescaled to 189 GeV, calculated from the fits to the mixed semi-leptonic samples built from the data and the MC. The values for $R_{\text{mixed SL MC}}$ are presented in Table 4, for the different models, along with the calibrated values of R_{4q} for the same models.

The calibration factors differ from unity by less than 6%, and the largest difference of the calibrated $R_{4q\,\text{MC}}$ values when changing the fragmentation model, 0.014, was considered as an estimate of the systematic error due to simulation of the fragmentation and of the detector response, and was added in quadrature to the systematic error. The error in the calibrated $R_{4q\,\text{MC}}$ values due to the statistical error on $\langle R_{\text{mixed SL Data}} \rangle$ value used for the calibration, 0.026, was also added in quadrature to the systematic error.

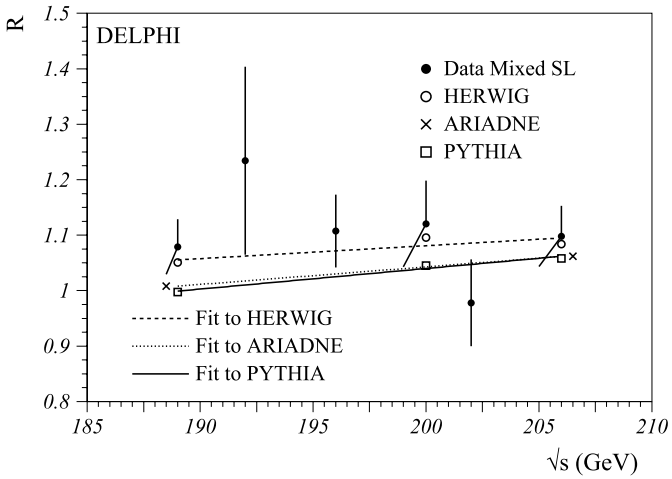

Fig. 8. The ratio $R_{\text{mixed SL}}$ as function of $\sqrt{s}$ for data and MC, and fits to the MC (see text). The ARIADNE *points* at 189 GeV and at 206 GeV have their centre-of-mass energy shifted and the *error bars* on data are tilted for readability

Table 4. Ratio of data to MC fitted values of R in mixed semi-leptonic samples, used to calibrate the $R_{4q\,\text{MC}}$ values for different models (upper line), and calibrated values of $R_{4q\,\text{MC}}$. All values were computed at $\sqrt{s} = 189$ GeV

MC sample	PYTHIA	ARIADNE	HERWIG
$R_{\text{mixed SL Data}}/$ $R_{\text{mixed SL MC}}$	1.053	1.044	0.997
$R_{4q\,\text{MC}}^{\text{Calibrated}}$	1.018	1.011	1.004

4.4.2 Bose–Einstein correlations

Bose–Einstein correlations (BEC) between identical pions and kaons are known to exist and were established and studied in Z hadronic decays in [35–54]. They are expected to exist with a similar behaviour in the W hadronic decays, and this is studied in [2]. They are implemented in the MC simulation samples with BEC via the BE_{32} model of LUBOEI [26], which was tuned to describe the DELPHI data in [2]. However, the situation for the WW (ZZ) fully hadronic decays is not so clear, i.e. whether there are correlations only between pions and kaons coming from the same $W(Z)$ boson or also between pions and kaons from different $W(Z)$ bosons. The analyses of Bose–Einstein correlations between identical particles coming from the decay of different W bosons do not show a significant effect [55–57] for three of the LEP experiments, whereas for DELPHI, an effect was found at the level of 2.4 standard deviations [2]. Thus, a comparison was made between the WPHACT samples without CR and with BEC only between the identical pions coming from the same W boson (BEC only inside), to the samples without CR and with BEC allowed for all the particles stemming from both W bosons, implemented with the BE_{32} variant of the LUBOEI model (BEC all). The R values were obtained at each centre-of-mass energy, after which a linear fit was performed for each model to obtain a best prediction at 189 GeV. The fit values were found to be in agreement to the estimate at 189 GeV alone, and for simplicity this estimate was used. The measurement of BEC from DELPHI of 2.4 standard deviations above zero (corresponding to BEC only inside), was used to interpolate the range of 4.1 standard deviations of separation between BEC only inside and BEC all. To include the error on the measured BEC effect, one standard deviation was added to the effect before the interpolation. The difference in the estimated values of R at $\sqrt{s} = 189$ GeV, between the model with BEC only inside and the model with partial BEC all (at the interpolated point of 3.4/4.1), -0.013, was added in quadrature to the systematic error.

4.4.3 $q\bar{q}(\gamma)$ background shape

The fragmentation effects, in the shape of the $q\bar{q}(\gamma)$ background, were estimated by comparing the values of R obtained when the subtracted $q\bar{q}(\gamma)$ sample was fragmented with ARIADNE instead of PYTHIA at the centre-of-mass energy of 189 GeV, and the difference, 0.003, was added in quadrature to the systematic error.

4.4.4 $q\bar{q}(\gamma)$ and ZZ background contribution

At the centre-of-mass energy of 189 GeV, the $q\bar{q}(\gamma)$ cross-section in the 4-jet region is poorly known, due to the difficulty in isolating the $q\bar{q}(\gamma) \to$ 4-jet signal from other 4-jet processes such as WW and ZZ. The study performed in [58] has shown that the maximal difference in the estimated $q\bar{q}(\gamma)$ background rate is 10% coming from changing from PYTHIA to HERWIG as the hadronization model, with the ARIADNE model giving intermediate results. Conservatively, at each centre-of-mass energy a variation of 10% on the $q\bar{q}(\gamma)$ cross-section was assumed, and the largest shift in R, 0.011, was added in quadrature to the systematic error.

The other background process considered is the Z pair production. The Standard Model predicted cross-sections are in agreement with the data at an error level of 10% [59]. The cross-section was thus varied by $\pm 10\%$ at each energy and the effect in R was found to be negligible.

4.4.5 Evolution of R with energy

The R ratios were rescaled to $\sqrt{s} = 189$ GeV using the fit to the MC without CR, however the correct behaviour might be given by the MC with CR. Hence, the difference of 0.009 between the R values obtained using the two rescaling methods, using MC without CR $\langle R \rangle$ and with CR $\langle R_{\text{CR rescale}} \rangle$, was added in quadrature to the systematic error.

4.5 Results of the particle flow analysis

The final result for the average of the ratios R rescaled to 189 GeV is

$$\langle R \rangle = 0.979 \pm 0.032\,(\text{stat}) \pm 0.035\,(\text{syst})\,. \qquad (8)$$

In order to facilitate comparisons between the four LEP experiments, this value can be normalised by the one determined from simulation samples produced with the full detector simulation and analysed with the same method. The LEP experiments agreed to use for this purpose the Cetraro PYTHIA samples. These events were generated with the ALEPH fragmentation tuning but have been reconstructed with the DELPHI detector simulation and analysed with this analysis. The values of the R ratios obtained from the Cetraro samples at 189 GeV, calibrated using the mixed semi-leptonic events from these samples, are given in Table 5.

The value of $\langle R \rangle$ measured from data is between the expected R ratios from PYTHIA without CR and with the SK-I model with 100% fraction of reconnection. The error of this measurement is larger than the difference between the values of R from ARIADNE samples without and with CR, and than the difference between values of R from the HERWIG samples without CR and with 1/9 of reconnected events.

The following normalised ratios are obtained for the sample without CR and implementing the SK-I model with 100% CR probability, respectively:

$$r^{\text{data}}_{\text{no CR}} = \frac{\langle R \rangle_{\text{data}}}{R_{\text{no CR}}} = 0.944 \pm 0.031\,(\text{stat}) \pm 0.034\,(\text{syst})\,, \tag{9}$$

$$r^{\text{data}}_{\text{CR}} = \frac{\langle R \rangle_{\text{data}}}{R_{\text{CR}}} = 1.067 \pm 0.035\,(\text{stat}) \pm 0.039\,(\text{syst})\,. \tag{10}$$

In the above expressions, the statistical errors in the MC predicted values were propagated and added quadratically to the systematic errors on the ratios.

It is also possible to define the following quantity, taking the predictions for R_{CR} and $R_{\text{no CR}}$ at $\sqrt{s} = 189$ GeV from the PYTHIA samples in Table 5,

$$\delta r = \frac{\langle R_{\text{data}} \rangle - R_{\text{no CR}}}{R_{\text{CR}} - R_{\text{no CR}}} = 0.49 \pm 0.27\,(\text{stat}) \pm 0.29\,(\text{syst})\,, \tag{11}$$

from which it can be concluded that the measured $\langle R_{\text{data}} \rangle$ is compatible with intermediate probability of CR, and differs from the CR in the SK-I model at 100% at the level of 1.3 standard deviations. The ability to distinguish between these two models can be computed from the inverse

Table 5. R ratios for the Cetraro samples at 189 GeV, calibrated with the mixed semi-leptonic events

MC Sample	R
PYTHIA no CR	1.037 ± 0.004
PYTHIA SK-I 100%	0.917 ± 0.003
ARIADNE no CR	1.053 ± 0.004
ARIADNE AR2	1.021 ± 0.004
HERWIG no CR	1.059 ± 0.004
HERWIG 1/9 CR	1.040 ± 0.003

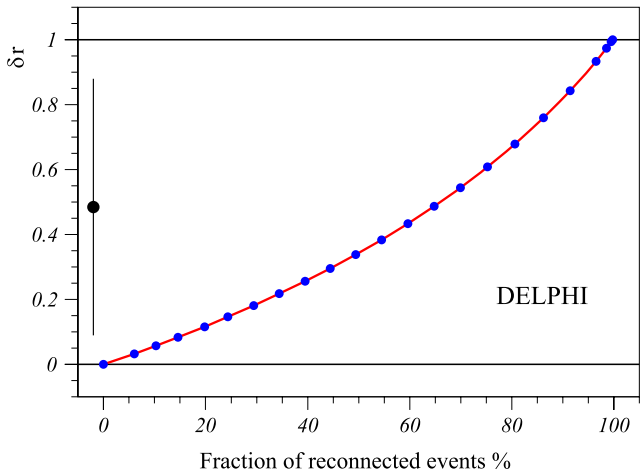

Fig. 9. Comparison of the measurement of the δr observable to the predictions from the SK-I model as a function of the fraction of reconnected events

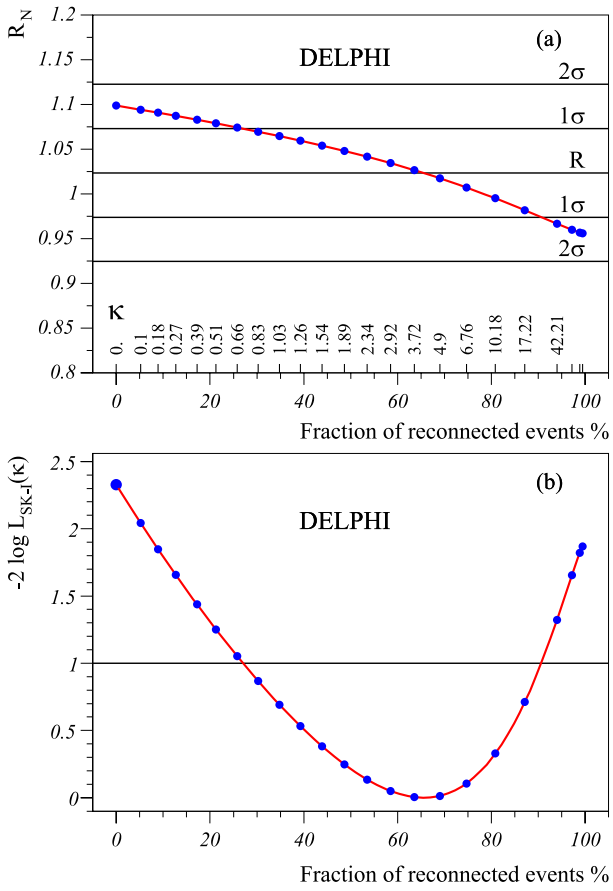

Fig. 10. a Estimated ratio R_N at 200 GeV plotted as a function of different κ values (*top scale*), or as function of the corresponding reconnection probabilities (*bottom scale*), compared to $\langle R \rangle$ measured from data after rescaling to 200 GeV (*horizontal lines* marked with R for the value and with $1\sigma(2\sigma)$ for the $\langle R \rangle$ value added/subtracted by one(two) standard deviations); the last three marks on the x axis, close to 100% of reconnection probability, correspond respectively to the values $\kappa = 100, 300, 800$; **b** corresponding log-likelihood curve for the comparison of the estimated values (R_N) with the data ($\langle R \rangle$)

of the sum in quadrature of the statistical and systematic errors; it amounts to be 2.5 standard deviations. In Fig. 9 the result of δr is compared to the predicted values, in the scope of the SK-I model, as a function of the fraction of reconnected events.

The result for the value of $\langle R \rangle$ can also be used to test for consistency with the SK-I model as a function of κ and a log-likelihood curve was obtained. This also facilitates combination with the result obtained in the analysis in the following section, and for this reason the value of $\langle R \rangle$ is rescaled with PYTHIA without CR to a centre-of-mass energy of 200 GeV: the value obtained at 200 GeV is $\langle R \rangle(200\,\text{GeV}) = 1.024 \pm 0.050$. The values obtained for the predicted ratios R_N at 200 GeV and the log-likelihood curve, as a function of κ, are shown in Fig. 10. The value of κ most compatible with the data within one standard deviation is

$$\kappa_{\text{SK-I}} = 4.13^{+20.97}_{-3.46}\,. \tag{12}$$

5 Different M_W estimators as observables

It has been shown [15] that the M_W measurement inferred from hadronically decaying W^+W^- events at LEP-2, by the method of direct reconstruction, is influenced by CR effects, most visible when changing the value of κ in the SK-I model. For the $M_W(4q)$ estimator within DELPHI this is shown in [60]. Other published M_W estimators in LEP experiments are equally sensitive to κ [61].

To probe this sensitivity to CR effects, alternative estimators for the M_W measurement were designed which have different sensitivity to κ. In the following, the standard estimator and two alternative estimators, studied in this paper, are presented. The standard estimator corresponds to that previously used in the measurement of the W mass by DELPHI [60]. Note that in the final DELPHI W mass analysis [62] results are given for the standard and hybrid cone estimators, with the hybrid cone estimator used to provide the primary result. The data samples, efficiencies and purities for the analysis corresponding to the standard estimator are provided in [60, 62].

- **The standard M_W estimator**: This estimator is described in [60] and was optimised to obtain the smallest statistical uncertainty for the W mass measurement. It results in an event-by-event likelihood $L_i(M_W)$ for the parameter M_W.
- **The momentum cut M_W estimator**: For this alternative M_W estimator the event selection was performed in exactly the same way as for the standard M_W estimator. The particle-jet association was also taken from this analysis. However, when reconstructing the event for the M_W extraction a tighter track selection was applied. The momentum and energy of the jets were calculated only from those tracks having a momentum higher than a certain p_{cut} value. An event-by-event likelihood $L_i^{p_{\text{cut}}}(M_W)$ was then calculated.
- **The hybrid cone M_W estimator**: In this second alternative M_W estimator the reconstruction of the event is the same as for the standard analysis, except when calculating the jet momenta used for the M_W extraction. An iterative procedure was used within each jet (defined by the clustering algorithm used in the standard analysis) to find a stable direction of a cone excluding some particles in the calculation of the jet momentum, illustrated in Fig. 11. Starting with the direction of the original jet $\mathbf{p}^{\text{jet}}_{\text{std}}$, the jet direction was recalculated (direction (1) on the Figure) only from those particles which have an opening angle smaller than R_{cone} with this original jet. This process was iterated by constructing a second cone (of the same opening angle) around this new jet direction and the jet direction was recalculated again. The iteration was continued until a stable jet direction $\mathbf{p}^{\text{jet}}_{\text{cone}}$ was found. The jet momenta obtained, $\mathbf{p}^{\text{jet}}_{\text{cone}}$, were rescaled to compensate for the lost energy of particles outside the stable cone,

$$\mathbf{p}^{\text{jet}}_{\text{cone}} \to \mathbf{p}^{\text{jet}}_{\text{cone}} \frac{E^{\text{jet}}}{E^{\text{jet}}_{\text{cone}}}\,. \tag{13}$$

The energies of the jets were taken to be the same as those obtained with the standard clustering algorithm ($E^{\text{jet}}_{\text{cone}} \to E^{\text{jet}}$). This was done to increase the correlation of this estimator with the standard one. The rescaling was not done for the p_{cut} estimator as it will be used in a cross-check observable with different systematic properties. Again the result is an event-by-event likelihood $L_i^{R_{\text{cone}}}(M_W)$.

Each of these previously defined M_W likelihoods had to be calibrated. The slope of the linear calibration curve for the M_W estimators is tuned to be unity, therefore only a bias correction induced by the reconstruction method has to be applied. This bias is estimated with the nominal WPHACT Monte Carlo events and the dependence on the value of κ is estimated with the EXCALIBUR simulation. It was verified for smaller subsets that the results using these large EXCALIBUR samples and the samples generated with WPHACT are compatible. Neglect-

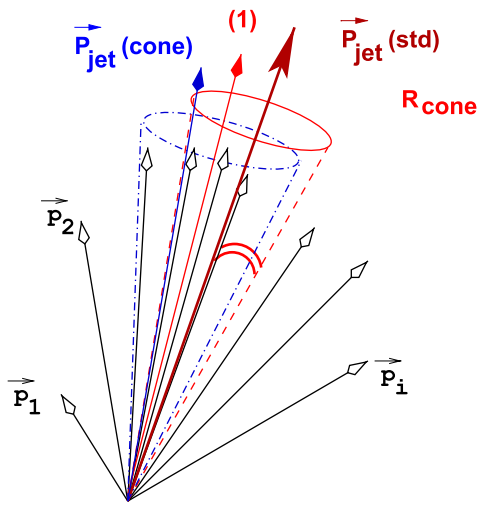

Fig. 11. Illustration of the iterative cone algorithm within a predefined jet as explained in the text

ing the possible existence of Colour Reconnection (CR) in the Monte Carlo simulation results in event likelihoods $L_i(M_W|\text{event without CR})$, while $L_i(M_W|\text{event with CR})$ are the event likelihoods obtained when assuming the hypothesis that events do reconnect (100% CR in the scope of the SK-I model). To construct the event likelihoods for intermediate CR (values of κ larger than 0) the following weighting formula is used:

$$L_i(M_W|\kappa) = [1-\mathcal{P}_i(\kappa)]L_i(M_W|\text{event without CR}) + \mathcal{P}_i(\kappa)L_i(M_W|\text{event with CR})\,, \quad (14)$$

where $\mathcal{P}_i(\kappa)$ is defined in (1). The combined likelihood is produced for the event sample; the calibrated values for $M_W(\kappa)$ were obtained for different values of κ using the maximum likelihood principle. In Fig. 12 the difference $\mathrm{d}M_W(\kappa) = M_W(\kappa) - M_W(\kappa=0)$ or the influence of κ on the bias of the M_W estimator is presented as function of κ.

The uncertainty on this difference is estimated with the Jackknife method [33] to take the correlation between $M_W(\kappa)$ and $M_W(\kappa=0)$ into account. It was observed from simulations that the estimators dependency on κ, for κ below about 5, was not significantly different in the centre-of-mass range between 189 and 207 GeV. Therefore in the determination of κ the dependency at 200 GeV was taken as default for all centre-of-mass energies. This value of centre-of-mass energy is close to the integrated luminosity weighted centre-of-mass energy of the complete data sample, which is 197.1 GeV.

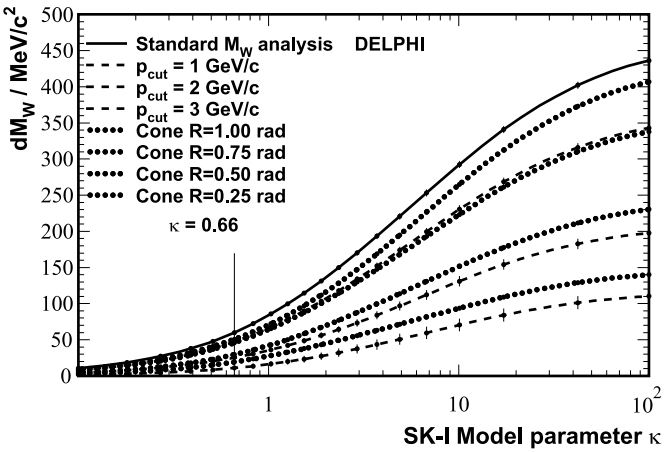

Fig. 12. The difference $\mathrm{d}M_W(\kappa) = M_W(\kappa) - M_W(\kappa=0)$ is presented as a function of κ, for different M_W estimators. The curve for the standard M_W estimator is the curve at the top. The curves obtained with the hybrid cone analysis for different values of the cone opening angle, starting from the top with 1.00 rad down to 0.75 rad, 0.50 rad and 0.25 rad are indicated with dotted lines. The curves obtained with the momentum cut analysis for different values of p_{cut}, starting from the top with 1 GeV/c, down to 2 GeV/c and 3 GeV/c are *dashed*. The *vertical line* indicates the value of κ preferred by the SK-I authors [5] and commonly used to estimate systematic uncertainties on measurements using $e^+e^- \to W^+W^- \to q_1\bar{q}_2q_3\bar{q}_4$ events

When neglecting the information content of low momentum particles or when using the hybrid cone algorithm, the influence of Colour Reconnection on the M_W estimator is decreased. The dependence $\frac{\partial M_W}{\partial \kappa}$ of the estimator to κ is decreased when increasing the value of p_{cut} or when working with smaller cone opening angles R_{cone}.

5.1 The measurement of κ

The observed difference $\Delta M_W(\mathrm{std}, i) = M_W^{\mathrm{std}} - M_W^i$ in the event sample, where i is a certain alternative analysis, provides a measurement of κ. When both estimators M_W^{std} and M_W^i are calibrated in the same hypothesis of κ, the expectation values of $\Delta M_W(\mathrm{std}, i)$ will be invariant under a change of p_{cut} or R_{cone}.

When neglecting part of the information content of the events in these alternative M_W analyses, by increasing p_{cut} or decreasing R_{cone}, the statistical uncertainty on the value of the M_W estimator is increased. Therefore a balance must be found between the statistical precision on $\Delta M_W(\mathrm{std}, i)$ and the dependence of this difference to κ in order to obtain the largest sensitivity for a κ measurement. This optimum was found using the Monte Carlo simulated events and assuming that the data follow the $\kappa = 0$ hypothesis, resulting in the smallest expected uncertainty on the estimation of κ.

For the p_{cut} analysis an optimal sensitivity was found when using the difference $\Delta M_W(\mathrm{std}, p_{\mathrm{cut}})$ with p_{cut} equal to 2 GeV/c or 3 GeV/c. Even more information about κ could be extracted from the data, when using the difference $\Delta M_W(\mathrm{std}, R_{\mathrm{cone}})$, which was found to have an optimal sensitivity around $R_{\mathrm{cone}} = 0.5$ rad. No significant improvement in the sensitivity was found when combining the information from these two observables. Therefore the best measure of κ using this method is extracted from the $\Delta M_W(\mathrm{std}, R_{\mathrm{cone}} = 0.5\,\mathrm{rad})$ observable. Nevertheless, the $\Delta M_W(\mathrm{std}, p_{\mathrm{cut}} = 2\,\mathrm{GeV}/c)$ observable was studied as a cross-check.

5.2 Study of the systematic errors in the ΔM_W method

The estimation of systematic uncertainties on the observables $\Delta M_W(\mathrm{std}, i)$ follows similar methods to those used within the M_W analysis. Here the double difference is a measure of the systematic uncertainty between Monte Carlo simulation (MC) and real data (DA):

$$\Delta_{\mathrm{syst}}(\mathrm{MC,\,DA}) = \big|[M_W^{\mathrm{std}}(\mathrm{MC}) - M_W^{\mathrm{std}}(\mathrm{DA})] - [M_W^i(\mathrm{MC}) - M_W^i(\mathrm{DA})]\big|\,, \quad (15)$$

where i is one of the alternative M_W estimators. The systematic error components are described below and summarised in Table 6.

5.2.1 Jet reconstruction systematics with MLBZs

A novel technique was proposed in [63] to study systematic uncertainties on jet reconstruction and fragmentation in W physics measurements with high statistical precision through the use of mixed Lorentz boosted Z events

Table 6. Breakdown of the total uncertainty on both relevant observables

Source	Uncertainty contribution (MeV/c^2) $\Delta M_W(\text{std}, R_{\text{cone}} = 0.5\,\text{rad})$	$\Delta M_W(\text{std}, p_{\text{cut}} = 2\,\text{GeV}/c)$
Fragmentation	11	27
Calibration	3	3
Background	3	3
BEI-BEA	8	9
Total systematic	14	29
Statistical Error	35	61
Total	38	67

(MLBZs). The technique is similar to the one described in Sect. 4.4.1. The main advantage of this method was that Monte Carlo simulated jet properties in W^+W^- events could be directly compared with the corresponding ones from real data using the large Z statistics.

The main extension of the method beyond that described in [63] consisted in an improved mixing and boosting procedure of the Z events into MLBZs, demonstrated in Fig. 13.

The 4-momenta of the four primary quarks in WPHACT generated $W^+W^- \to q_1\bar{q}_2q_3\bar{q}_4$ events were used as event templates. The Z events from data or simulation were chosen such that their thrust axis directions were close in polar angle to one of the primary quarks of

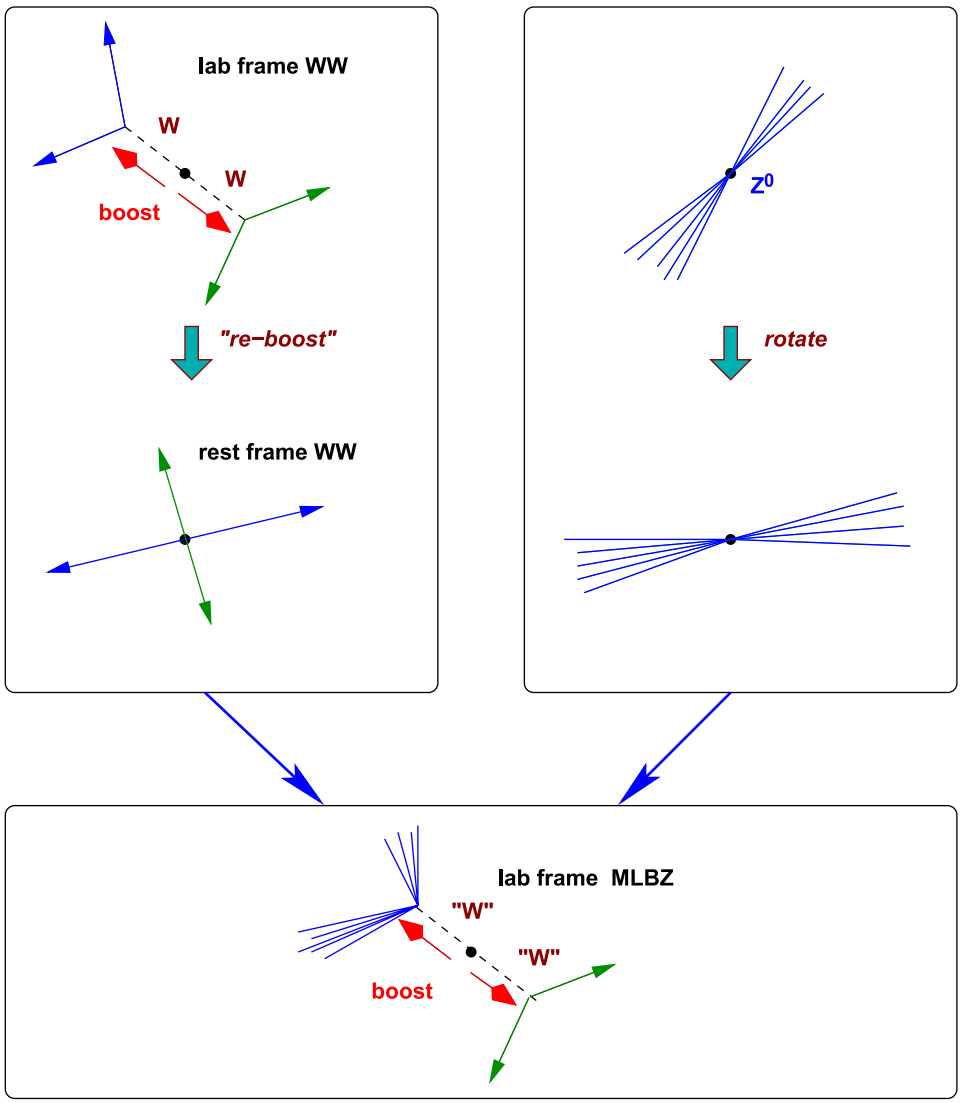

Fig. 13. Illustration of the mixing and boosting procedure within the MLBZ method (see text for details)

the W^+W^- event template. Each template W was then boosted to its rest frame. The particles in the final state of a selected Z event were rotated so that the thrust axis matches the rest frame direction of the primary quarks in the W^+W^- template. After rescaling the kinematics of the Z events to match the W boson mass in the generated W^+W^- template, the two Z events were boosted to the lab frame of the W^+W^- template. All particles having an absolute polar angle with the beam direction smaller than 11° were removed from the event. The same generated WPHACT events were used for the construction of both the data MLBZs and Monte Carlo MLBZs in order to increase the correlation between both emulated samples to about 31%. This correlation was taken into account when quoting the statistical uncertainty on the systematic shift on the observables between data and Monte Carlo MLBZs.

It was verified that when introducing a significant mass shift of 300 MeV/c^2 on M_W by using the cone rejection algorithm, it was reproduced within 15% by applying the MLBZ technique. Because the expected systematic uncertainties on the $\Delta M_W(\mathrm{std}, i)$ observables of interest are one order of magnitude smaller than 300 MeV/c^2, this method is clearly justified.

The double difference of (15) was determined with the MLBZ method using Z events selected in the data sets collected during the 1998 calibration runs and Z events from the corresponding Monte Carlo samples. The following results were obtained for the $\Delta M_W(\mathrm{std}, R_{\mathrm{cone}} = 0.5\,\mathrm{rad})$ observable:

$$\begin{aligned} \Delta_{\mathrm{syst}}(\mathrm{ARIADNE,\,DA}) &= -1.9 \pm 3.9\,(\mathrm{stat})\,\mathrm{MeV}/c^2 \\ \Delta_{\mathrm{syst}}(\mathrm{PYTHIA,\,DA}) &= -5.7 \pm 3.9\,(\mathrm{stat})\,\mathrm{MeV}/c^2 \\ \Delta_{\mathrm{syst}}(\mathrm{HERWIG,\,DA}) &= -10.6 \pm 3.9\,(\mathrm{stat})\,\mathrm{MeV}/c^2\,, \end{aligned} \tag{16}$$

where the statistical uncertainty takes into account the correlation between the Monte Carlo and the data MLBZ events, together with the correlation between the two M_W estimators. This indicates that most of the fragmentation, detector and Between-W Bose–Einstein correlation systematics are small. The study was not performed for the $\Delta M_W(\mathrm{std}, p_{\mathrm{cut}})$ observable.

Other systematic sources on the reconstructed jets are not considered as the M_W estimators used in the difference $\Delta M_W(\mathrm{std}, i)$ have a large correlation.

5.2.2 Additional fragmentation systematic study

The fragmentation of the primary partons is modelled in the Monte Carlo simulation used for the calibration of the M_W^i observables.

The expected values on the M_W estimators from simulation (in the $\kappa = 0$ hypothesis) are changed when using different fragmentation models [60], resulting in systematic uncertainties on the measured M_W^i observables and hence possibly also on our estimated κ. In Fig. 14 the systematic shift δM_W in the different M_W^i observables is shown when using HERWIG or ARIADNE rather than PYTHIA as the fragmentation model in the no Colour Reconnection hypothesis. When inferring κ from the data difference, $\Delta M_W(\mathrm{std}, i)$, the PYTHIA model is used to calibrate each M_W^i observable. This data difference for $M_W^{p_{\mathrm{cut}}=2\ \mathrm{GeV}/c}$, $\Delta M_W(\mathrm{std}, p_{\mathrm{cut}} = 2\,\mathrm{GeV}/c)$, changes[3] by $(27 \pm 12)\,\mathrm{MeV}/c^2$ or $(8 \pm 12)\,\mathrm{MeV}/c^2$ when replacing PYTHIA by respectively HERWIG or ARIADNE. Similarly, the observable $\Delta M_W(\mathrm{std}, R_{\mathrm{cone}} = 0.5\,\mathrm{rad})$ changes by $(-4 \pm 10)\,\mathrm{MeV}/c^2$ or $(-6 \pm 10)\,\mathrm{MeV}/c^2$ when replacing PYTHIA by respectively HERWIG or ARIADNE. The largest shift of the observable when changing fragmentation models (or the uncertainty on this shift if larger) is taken as systematic uncertainty on the value of the observable. Hence, systematic errors of 27 MeV/c^2 for the $\Delta M_W(\mathrm{std}, p_{\mathrm{cut}} = 2\,\mathrm{GeV}/c)$ observable and 10 MeV/c^2 for the $\Delta M_W(\mathrm{std}, R_{\mathrm{cone}} = 0.5\,\mathrm{rad})$ observable were assumed as the contribution from fragmentation uncertainties. The MLBZ studies (see above) are compatible with these results, hence no additional systematic due to fragmentation was quoted for the $\Delta M_W(\mathrm{std}, R_{\mathrm{cone}} = 0.5\,\mathrm{rad})$ observable.

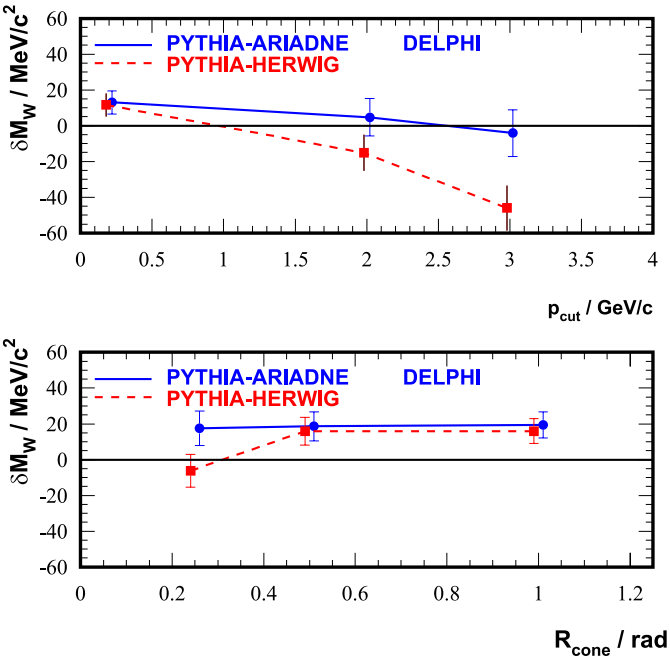

Fig. 14. Systematic shifts δM_W, on M_W observables, when applying different fragmentation models as a function of the p_{cut} or R_{cone} values used in the construction of the M_W observable. These Monte Carlo estimates were obtained at a centre-of-mass energy of 189 GeV. The uncertainties are determined with the Jackknife method

5.2.3 Energy dependence

The biases of the different M_W estimators have a different dependence on the centre-of-mass energy, hence the calibration of $\Delta M_W(i, j)$ will be energy dependent.

[3] This change, $\Delta M_W(\mathrm{std}, p_{\mathrm{cut}} = 2\,\mathrm{GeV}/c)^{\mathrm{PYTHIA}} - \Delta M_W(\mathrm{std}, p_{\mathrm{cut}} = 2\,\mathrm{GeV}/c)^{\mathrm{HERWIG}}$, is given by $\delta M_W(\mathrm{std} \equiv p_{\mathrm{cut}} = 0.2\,\mathrm{GeV}/c)^{\mathrm{PYTHIA-HERWIG}} - \delta M_W(p_{\mathrm{cut}} = 2\,\mathrm{GeV}/c)^{\mathrm{PYTHIA-HERWIG}}$, and similar expressions for the ARIADNE and R_{cone} cases (for R_{cone}, $\mathrm{std} \equiv R_{\mathrm{cone}} = \pi$).

The energy dependence of each individual M_W estimator was parameterised with a second order polynomial. Since WPHACT event samples were used at a range of centre-of-mass energies the uncertainty on the parameters describing these curves are small. Therefore a small systematic uncertainty of $3\,\mathrm{MeV}/c^2$ was quoted on the $\Delta M_W(i,j)$ observables due to the calibration.

5.2.4 Background

The same event selection criteria were applied for all the M_W estimators, hence the same background contamination is present in all analyses. The influence of the $q\bar{q}(\gamma)$ background events on the individual M_W estimators is small [60] and was taken into account when constructing the centre-of-mass energy dependent calibration curves of the individual M_W estimators. The residual systematic uncertainty on both $\Delta M_W(i,j)$ observables is $3\,\mathrm{MeV}/c^2$.

5.2.5 Bose–Einstein correlations

As for the particle flow method, the systematic uncertainties due to possible Bose–Einstein correlations are estimated via Monte Carlo simulations. The relevant values for the systematic uncertainties on the observables are the differences between the observables obtained from the Monte Carlo events with Bose–Einstein correlations inside individual W's (BEI) and those with, in addition, Bose–Einstein correlations between identical particles from different W's (BEA). The values were estimated to be $(6.4 \pm 9.3)\,\mathrm{MeV}/c^2$ for the $\Delta M_W(\mathrm{std}, p_{\mathrm{cut}} = 2\,\mathrm{GeV}/c)$ observable, and $(7.2 \pm 8.2)\,\mathrm{MeV}/c^2$ for the $\Delta M_W(\mathrm{std}, R_{\mathrm{cone}} = 0.5\,\mathrm{rad})$ observable. As the uncertainties in the estimated contributions were larger than the contributions themselves, these uncertainties were added in quadrature to the systematic errors on the relevant observables.

5.2.6 Cross-check in the semi-leptonic channel

Colour Reconnection between the decay products originating from different W boson decays can only occur in the $W^+W^- \to q_1\bar{q}_2 q_3 \bar{q}_4$ channel. The semi-leptonic W^+W^- decay channel (i.e, $q\bar{q}'\ell\overline{\nu}_\ell$) is by definition free of those effects. Therefore the determination of Colour Reconnection sensitive observables, like $\Delta M_W(\mathrm{std}, R_{\mathrm{cone}} = 0.5\,\mathrm{rad})$, in this decay channel could indicate the possible presence of residual systematic effects. A study of the $\Delta M_W(\mathrm{std}, R_{\mathrm{cone}} = 0.5\,\mathrm{rad})$ observable was performed in the semi-leptonic decay channel. The semi-leptonic M_W analysis in [60] was used and the cone algorithm was implemented in a similar way as for the fully hadronic decay channel. The same data sets have been used as presented throughout this paper and the following result was obtained:

$$\begin{aligned}\Delta M_W(\mathrm{std}, R_{\mathrm{cone}}) &= M_W^{\mathrm{std}} - M_W^{R_{\mathrm{cone}}} \\ &= (8 \pm 56\,(\mathrm{stat}))\,\mathrm{MeV}/c^2\,, \end{aligned} \quad (17)$$

where the statistical uncertainty was computed taking into account the correlation between both measurements. Although the statistical significance of this cross-check is small, a good agreement was found for both M_W estimators.

5.3 Results from the M_W estimators analyses

The observable $\Delta M_W(\mathrm{std}, R_{\mathrm{cone}})$ with R_{cone} equal to 0.5 rad (defined above), was found to be the most sensitive to the SK-I colour reconnection model, and the $\Delta M_W(\mathrm{std}, p_{\mathrm{cut}} = 2\,\mathrm{GeV}/c)$ observable was measured as a cross-check. The analyses were calibrated with PYTHIA $\kappa = 0$ WPHACT generated simulation events. The values measured from the combined DELPHI data at centre-of-mass energies ranging between 183 and 208 GeV are:

$$\begin{aligned}\Delta M_W(\mathrm{std}, R_{\mathrm{cone}}) &= M_W^{\mathrm{std}} - M_W^{R_{\mathrm{cone}}} \\ &= (59 \pm 35\,(\mathrm{stat}) \pm 14\,(\mathrm{syst}))\,\mathrm{MeV}/c^2 \\ \Delta M_W(\mathrm{std}, p_{\mathrm{cut}}) &= M_W^{\mathrm{std}} - M_W^{p_{\mathrm{cut}}} \\ &= (143 \pm 61\,(\mathrm{stat}) \pm 29\,(\mathrm{syst}))\,\mathrm{MeV}/c^2\,, \end{aligned} \quad (18)$$

where the first uncertainty numbers represent the statistical components and the second the combined systematic ones. The full breakdown of the uncertainties on both observables can be found in Table 6.

From these values estimates were made for the κ parameter by comparing them with the Monte Carlo expected values in different hypothesis of κ, shown in Fig. 15 for the observable $\Delta M_W(\mathrm{std}, R_{\mathrm{cone}} = 0.5\,\mathrm{rad})$.

The Gaussian uncertainty on the measured observables was used to construct a log-likelihood function $\mathcal{L}(\kappa) = -2\log L(\kappa)$ for κ. The log-likelihood function obtained is shown in Fig. 16 for the first and in Fig. 17 for the second observable.

The result shown in Fig. 16 is the primary result of this analysis, because of the larger sensitivity of the $\Delta M_W(\mathrm{std}, R_{\mathrm{cone}} = 0.5\,\mathrm{rad})$ observable to the value of κ

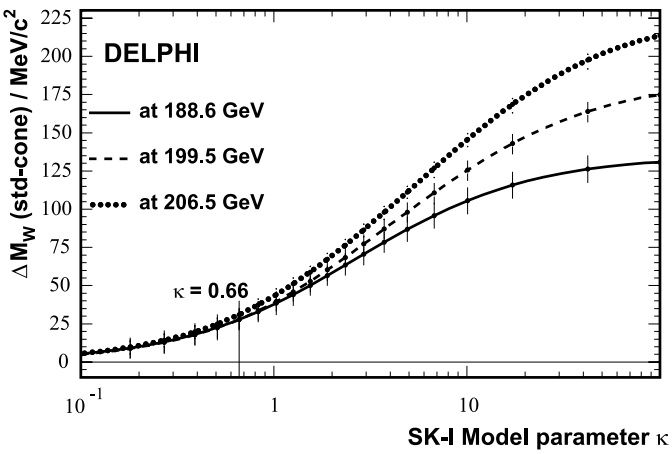

Fig. 15. The dependence of the observable $\Delta M_W(\mathrm{std}, R_{\mathrm{cone}} = 0.5\,\mathrm{rad})$ from simulation events on the value of the SK-I model parameter κ. The dependence is given at three centre-of-mass energies

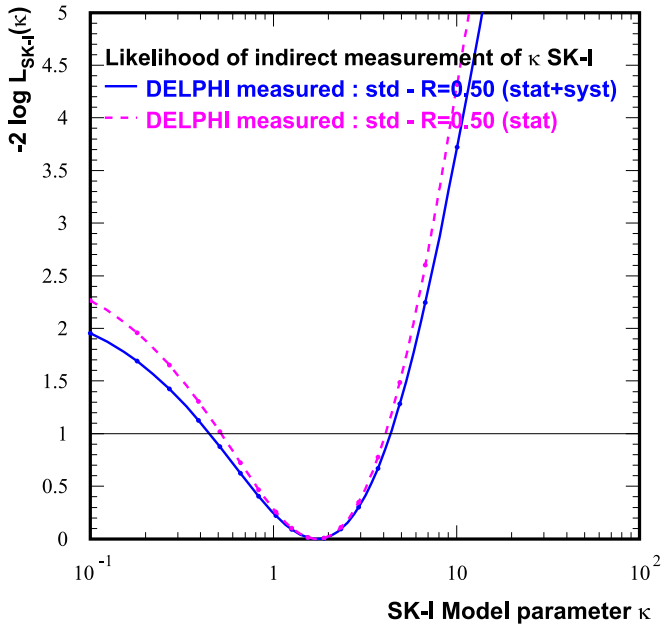

Fig. 16. The log-likelihood function $-2\log L(\kappa)$ obtained from the DELPHI data measurement of $\Delta M_W(\mathrm{std}, R_{\mathrm{cone}} = 0.5\,\mathrm{rad})$. The *bottom curve* (*full line*) gives the final result including the statistical uncertainty on $\Delta M_W(\mathrm{std}, R_{\mathrm{cone}} = 0.5\,\mathrm{rad})$ and the investigated systematic uncertainty contributions. The *top curve* (*dashed*) is centred on the same minimum and reflects the log-likelihood function obtained when only statistical uncertainties are taken into account

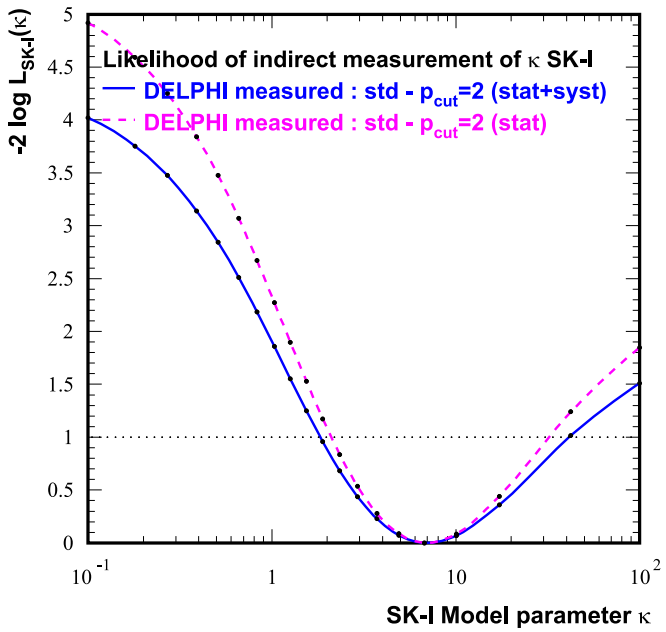

Fig. 17. The log-likelihood function $-2\log L(\kappa)$ obtained from the DELPHI data measurement of $\Delta M_W(\mathrm{std}, p_{\mathrm{cut}} = 2\,\mathrm{GeV}/c)$. The *bottom curve* (*full line*) gives the final result including the statistical uncertainty on $\Delta M_W(\mathrm{std}, p_{\mathrm{cut}} = 2\,\mathrm{GeV}/c)$ and the investigated systematic uncertainty contributions. The *top curve* (*dashed*) is centred on the same minimum and reflects the log-likelihood function obtained when only statistical uncertainties are taken into account

(see Sect. 5.1). The value of κ most compatible with the data within one standard deviation of the measurement is

$$\kappa_{\mathrm{SK\text{-}I}} = 1.75^{+2.60}_{-1.30}\,. \tag{19}$$

The result on κ extracted from the cross-check $\Delta M_W(\mathrm{std}, p_{\mathrm{cut}} = 2\,\mathrm{GeV}/c)$ observable is found not to differ significantly from the quoted result obtained with the more optimal $\Delta M_W(\mathrm{std}, R_{\mathrm{cone}} = 0.5\,\mathrm{rad})$ observable. The significance can be determined by the difference between both M_W estimators:

$$M_W^{p_{\mathrm{cut}}} - M_W^{R_{\mathrm{cone}}} = (-84 \pm 59\,(\mathrm{stat}))\,\mathrm{MeV}/c^2\,. \tag{20}$$

Taking into account that the expectation of this difference depends on κ, we find a statistical deviation of about 1 to 1.5σ between the measurements. No improved sensitivity is obtained by combining the information of both observables.

In this paper the SK-I model for Colour Reconnection implemented in PYTHIA was studied because it parameterizes the effect as function of the model parameter κ. Other phenomenological models implemented in the ARIADNE [8–10] and HERWIG [6, 7] Monte Carlo fragmentation schemes exist and are equally plausible. Unfortunately their effect in $W^+W^- \to q_1\bar{q}_2q_3\bar{q}_4$ events cannot be scaled with a model parameter, analogous to κ in SK-I, without affecting the fragmentation model parameters. Despite this non-factorization property, the consistency of these models with the data can still be examined. The Monte Carlo predictions of the observables in the hypothesis with Colour Reconnection (calibrated in the hypothesis of no Colour Reconnection) give the following values:

$$\begin{aligned}
\mathrm{ARIADNE} &\to M_W^{\mathrm{std}} - M_W^{R_{\mathrm{cone}}} = (7.2 \pm 4.1)\,\mathrm{MeV}/c^2\\
\mathrm{ARIADNE} &\to M_W^{\mathrm{std}} - M_W^{p_{\mathrm{cut}}} = (9.4 \pm 7.0)\,\mathrm{MeV}/c^2\\
\mathrm{HERWIG} &\to M_W^{\mathrm{std}} - M_W^{R_{\mathrm{cone}}} = (19.7 \pm 4.0)\,\mathrm{MeV}/c^2\\
\mathrm{HERWIG} &\to M_W^{\mathrm{std}} - M_W^{p_{\mathrm{cut}}} = (22.8 \pm 6.9)\,\mathrm{MeV}/c^2\,.
\end{aligned} \tag{21}$$

The small effects on the observables with the HERWIG implementation of Colour Reconnection compared to those predicted by SK-I are due to the fact that the fraction of events that reconnect is smaller in HERWIG (1/9) compared to SK-I ($\gtrsim 25\%$ at $\sqrt{s} = 200\,\mathrm{GeV}$). After applying this scale factor between both models, their predicted effect on the W mass and on the $\Delta M_W(i, j)$ observables becomes compatible. The ARIADNE implementation of Colour Reconnection has a much smaller influence on the observables compared to those predicted with the SK-I and HERWIG Monte Carlo.

5.4 Correlation with direct M_W measurement

When using a data observable to estimate systematic uncertainties on some measurand inferred from the same data sample, the correlation between the estimator used to measure the systematic bias and the estimator of the absolute value of the measurand should be taken into account.

Therefore the correlation between the Colour Reconnection sensitive observables $\Delta M_W(\mathrm{std}, R_{\mathrm{cone}} = 0.5\,\mathrm{rad})$ and $\Delta M_W(\mathrm{std}, p_{\mathrm{cut}} = 2\,\mathrm{GeV}/c)$ and the absolute $M_W(\mathrm{std})$ estimator was calculated. The correlation was determined from the Monte Carlo events and with $\kappa = 0$ or no Colour Reconnection. The values obtained were found to be stable as a function of κ within the statistical precision. The correlation between $\Delta M_W(\mathrm{std}, R_{\mathrm{cone}} = 0.5\,\mathrm{rad})$ and $M_W(\mathrm{std})$ was found to be 11%, while for the one between $\Delta M_W(\mathrm{std}, p_{\mathrm{cut}} = 2\,\mathrm{GeV}/c)$ and $M_W(\mathrm{std})$ a value of 8% was obtained. Also the correlation between the different M_W estimators was estimated and found to be stable with the value of κ. A value of 83% was obtained for the correlation between $M_W(\mathrm{std})$ and $M_W^{R_{\mathrm{cone}}=0.5\,\mathrm{rad}}$, while 66% was obtained between $M_W(\mathrm{std})$ and $M_W^{p_{\mathrm{cut}}=2\,\mathrm{GeV}/c}$.

6 Combination of the results in the scope of the SK-I model

The log-likelihood curve from the particle flow method was combined with the curve from the ΔM_W method and the result is shown in Fig. 18. The correlations between the analyses were neglected because the overlap between the samples is small and the nature of the analyses is very different. The total errors were used (statistical and systematic added in quadrature) in the combination.

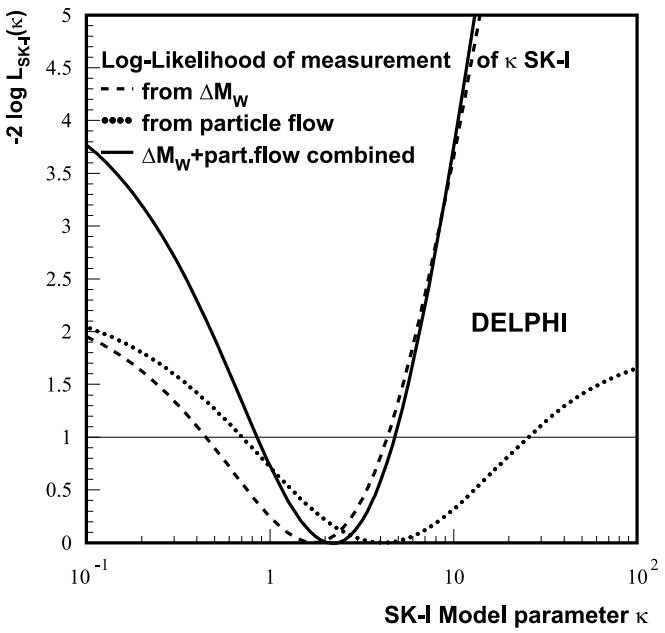

Fig. 18. The log-likelihood function $-2\log L(\kappa)$ obtained from the combined DELPHI measurement via $\Delta M_W(\mathrm{std}, R_{\mathrm{cone}} = 0.5\,\mathrm{rad})$ and the particle flow. The *full line* gives the final result including the statistical and systematic uncertainties. The log-likelihood functions are combined in the hypothesis of no correlation between the statistical and systematic uncertainties of both measurements

The best value for κ from the minimum of the curve, with its error given by the width of the curve at the value $-2\log L = (-2\log L)_{\min} + 1$, is:

$$\kappa_{\text{SK-I}} = 2.2^{+2.5}_{-1.3}\,. \tag{22}$$

7 Conclusions

Colour Reconnection (CR) effects in the fully hadronic decays of W pairs, produced in the DELPHI experiment at LEP, were investigated using the methods of the particle flow and the M_W estimators, notably the $\Delta M_W(\mathrm{std}, R_{\mathrm{cone}} = 0.5\,\mathrm{rad})$ observable.

The average of the ratios R of the integrals between 0.2 and 0.8 of the particle distribution in Inside-W regions to the Between-W regions was found to be

$$\langle R \rangle = 0.979 \pm 0.032\,(\mathrm{stat}) \pm 0.035\,(\mathrm{syst})\,. \tag{23}$$

The values used in this average were obtained after rescaling the value at each energy to the value at a centre-of-mass energy of 189 GeV using a fit to the MC without CR.

The effects of CR on the values of the reconstructed mass of the W boson, as implemented in different Monte Carlo models, were studied with different estimators. From the estimator of the W mass with the strongest sensitivity to the SK-I model of CR, the $\Delta M_W(\mathrm{std}, R_{\mathrm{cone}} = 0.5\,\mathrm{rad})$ method, the difference in data was found to be

$$\begin{aligned}\Delta M_W(\mathrm{std}, R_{\mathrm{cone}}) &= M_W^{\mathrm{std}} - M_W^{R_{\mathrm{cone}}=0.5\,\mathrm{rad}} \\ &= (59 \pm 35\,(\mathrm{stat}) \pm 14\,(\mathrm{syst}))\,\mathrm{MeV}/c^2\,.\end{aligned} \tag{24}$$

From the combination of the results from particle flow and M_W estimators, corresponding to the curve in full line shown in Fig. 18, the best value and total error for the κ parameter in the SK-I model was extracted to be:

$$\kappa_{\text{SK-I}} = 2.2^{+2.5}_{-1.3} \tag{25}$$

which corresponds to a probability of reconnection of $\mathcal{P}_{\mathrm{reco}} = 52\%$ and lies in the range $31\% < \mathcal{P}_{\mathrm{reco}} < 68\%$ at 68% confidence level.

The two analysis methods used in this paper are complementary: the method of particle flow provides a model-independent measurement but has significantly less sensitivity towards the SK-I model of CR than the method of ΔM_W estimators.

The obtained value of κ in (25) can be compared with similar values obtained by other LEP experiments, and it was found to be compatible with, but higher than, the values obtained with the particle flow by L3 [64] and OPAL [65]. It is also compatible with, but higher than, the values obtained with the method of different M_W estimators by OPAL [66] and ALEPH [67].

Acknowledgements. We thank the ALEPH Collaboration for the production of the simulated "Cetraro Samples".

We are greatly indebted to our technical collaborators, to the members of the CERN-SL Division for the excellent performance of the LEP collider, and to the funding agencies for their support in building and operating the DELPHI detector.

We acknowledge in particular the support of Austrian Federal Ministry of Education, Science and Culture, GZ 616.364/2-III/2a/98, FNRS–FWO, Flanders Institute to encourage scientific and technological research in the industry (IWT) and Belgian Federal Office for Scientific, Technical and Cultural affairs (OSTC), Belgium, FINEP, CNPq, CAPES, FUJB and FAPERJ, Brazil, Czech Ministry of Industry and Trade, GA CR 202/99/1362, Commission of the European Communities (DG XII), Direction des Sciences de la Matiére, CEA, France, Bundesministerium für Bildung, Wissenschaft, Forschung und Technologie, Germany, General Secretariat for Research and Technology, Greece, National Science Foundation (NWO) and Foundation for Research on Matter (FOM), The Netherlands, Norwegian Research Council, State Committee for Scientific Research, Poland, SPUB-M/CERN/PO3/DZ296/2000, SPUB-M/CERN/PO3/DZ297/2000, 2P03B 104 19 and 2P03B 69 23(2002-2004) FCT - Fundação para a Ciência e Tecnologia, Portugal, Vedecka grantova agentura MS SR, Slovakia, Nr. 95/5195/134, Ministry of Science and Technology of the Republic of Slovenia, CICYT, Spain, AEN99-0950 and AEN99-0761, The Swedish Research Council, Particle Physics and Astronomy Research Council, UK, Department of Energy, USA, DE-FG02-01ER41155, EEC RTN contract HPRN-CT-00292-2002.

References

1. G. Gustafson, U. Pettersson, P.M. Zerwas, Phys. Lett. B **209**, 90 (1988)
   x
2. DELPHI Collaboration, J. Abdallah et al., Eur. Phys. J. C **44**, 161 (2005)
3. V. Khoze, L. Lönnblad, R. Møller, T. Sjöstrand, Š. Todorova, N.K. Watson, in: Physics at LEP-2, Yellow Report CERN 96-01, ed. by G. Altarelli, T. Sjöstrand, F. Zwirner, **1**, 191 (1996)
4. The LEP Collaborations ALEPH, DELPHI, L3, OPAL, and the LEP W Working Group, Combined Preliminary Results on Colour Reconnection using Particle Flow in $e^+e^- \to W^+W^-$, note LEPEWWG/FSI/2002-01, ALEPH 2002-027 PHYSIC 2002-016, DELPHI 2002-090 CONF 623, L3 note 2768, and OPAL TN-724, July 17th, 2002, contribution to the summer Conferences of 2002, available at http://delphiwww.cern.ch/pubxx/delnote/public/2002_090_conf_623.ps.gz
5. T. Sjöstrand, V.A. Khoze, Z. Phys. C **62**, 281 (1994)
6. G. Marchesini et al., Comput. Phys. Commun. **67**, 465 (1992)
7. G. Corcella et al., JHEP **0101**, 010 (2001)
8. L. Lönnblad, Comput. Phys. Commun. **71**, 15 (1992)
9. H. Kharraziha, L. Lönnblad, Comput. Phys. Commun. **123**, 153 (1999)
10. G. Gustafson, J. Häkkinen, Z. Phys. C **64**, 659 (1994)
11. L. Lönnblad, Z. Phys. C **70**, 107 (1996)
12. DELPHI Collaboration, P. Abreu et al., Phys. Lett. B **416**, 233 (1998)
13. DELPHI Collaboration, P. Abreu et al., Eur. Phys. J. C **18**, 203 (2000) [Eur. Phys. J. C **25**, 493 (2002), Erratum]
14. D. Duchesneau, New Method Based on Energy and Particle Flow in $e^+e^- \to W^+W^- \to$ Hadrons Events for Colour Reconnection Studies, LAPP-EXP-2000-02 (http://wwwlapp.in2p3.fr/preplapp/LAPP_EX2000_02.pdf), presented at Workshop on WW Physics at LEP-200 (WW99), Kolymbari, Chania, Greece, 20–23 Oct 1999
15. J. D'Hondt, N.J. Kjaer, Measurement of Colour Reconnection Model Parameters Using M_W Analyses, contributed paper for ICHEP'02 (Amsterdam), note DELPHI 2002-048 CONF 582, available at http://delphiwww.cern.ch/pubxx/delnote/public/2002_048_conf_582.ps.gz
16. DELPHI Collaboration, P.A. Aarnio et al., Nucl. Instrum. Methods A **303**, 233 (1991)
17. DELPHI Collaboration, P. Abreu et al., Nucl. Instrum. Methods A **378**, 57 (1996)
18. DELPHI Trigger Group, A. Augustinus et al., Nucl. Instrum. Methods A **515**, 782 (2003)
19. DELPHI Silicon Tracker Group, P. Chochula et al., Nucl. Instrum. Methods A **412**, 304 (1998)
20. A. Ballestrero, R. Chierici, F. Cossutti, E. Migliore, Comput. Phys. Commun. **152**, 175 (2003)
21. E. Accomando, A. Ballestrero, Comput. Phys. Commun. **99**, 270 (1997)
22. E. Accomando, A. Ballestrero, E. Maina, Comput. Phys. Commun. **150**, 166 (2003)
23. T. Sjöstrand, Comput. Phys. Commun. **82**, 74 (1994)
24. T. Sjöstrand et al., Comput. Phys. Commun. **135**, 238 (2001)
25. DELPHI Collaboration, P. Abreu et al., Z. Phys. C **73**, 11 (1996)
26. L. Lönnblad, T. Sjöstrand, Eur. Phys. J. C **2**, 165 (1998)
27. F.A. Berends, R. Pittau, R. Kleiss, Comput. Phys. Commun. **85**, 437 (1995)
28. S. Jadach, B.F.L. Ward, Z. Was, Phys. Lett. B **449**, 97 (1999)
29. S. Jadach, B.F.L. Ward, Z. Was, Comput. Phys. Commun. **130**, 260 (2000)
30. S. Jadach et al., Comput. Phys. Commun. **140**, 475 (2001)
31. P. Abreu et al., Nucl. Instrum. Methods A **427**, 487 (1999)
32. S. Catani et al., Phys. Lett. B **269**, 432 (1991)
33. B. Efron, SIAM Rev. **21**, 460 (1979)
34. DELPHI Collaboration, J. Abdallah et al., Eur. Phys. J. C **34**, 399 (2004)
35. DELPHI Collaboration, P. Abreu et al., Phys. Lett. B **286**, 201 (1992)
36. DELPHI Collaboration, P. Abreu et al., Z. Phys. C **63**, 17 (1994)
37. DELPHI Collaboration, P. Abreu et al., Phys. Lett. B **355**, 415 (1995)
38. DELPHI Collaboration, P. Abreu et al., Phys. Lett. B **471**, 460 (2000)
39. L3 Collaboration, P. Achard et al., Phys. Lett. B **524**, 55 (2002)
40. L3 Collaboration, P. Achard et al., Phys. Lett. B **540**, 185 (2002)
41. OPAL Collaboration, P.D. Acton et al., Phys. Lett. B **267**, 143 (1991)
42. OPAL Collaboration, P.D. Acton et al., Phys. Lett. B **287**, 401 (1992)
43. OPAL Collaboration, P.D. Acton et al., Phys. Lett. B **298**, 456 (1993)

44. OPAL Collaboration, R. Akers et al., Z. Phys. C **67**, 389 (1995)
45. OPAL Collaboration, G. Alexander et al., Z. Phys. C **72**, 389 (1996)
46. OPAL Collaboration, K. Ackerstaff et al., Eur. Phys. J. C **5**, 239 (1998)
47. OPAL Collaboration, G. Abbiendi et al., Eur. Phys. J. C **11**, 239 (1999)
48. OPAL Collaboration, G. Abbiendi et al., Eur. Phys. J. C **16**, 423 (2000)
49. OPAL Collaboration, G. Abbiendi et al., Eur. Phys. J. C **21**, 23 (2001)
50. OPAL Collaboration, G. Abbiendi et al., Phys. Lett. B **523**, 35 (2001)
51. OPAL Collaboration, G. Abbiendi et al., Phys. Lett. B **559**, 131 (2003)
52. ALEPH Collaboration, D. Decamp et al., Z. Phys. C **54**, 75 (1992)
53. ALEPH Collaboration, A. Heister et al., Eur. Phys. J. C **36**, 147 (2004)
54. ALEPH Collaboration, S. Schael et al., Phys. Lett. B **611**, 66 (2005)
55. L3 Collaboration, P. Achard et al., Phys. Lett. B **547**, 139 (2002)
56. OPAL Collaboration, G. Abbiendi et al., Eur. Phys. J. C **36**, 297 (2004)
57. ALEPH Collaboration, S. Schael et al., Phys. Lett. B **606**, 265 (2005)
58. DELPHI Collaboration, J. Abdallah et al., Eur. Phys. J. C **34**, 127 (2004)
59. DELPHI Collaboration, J. Abdallah et al., Eur. Phys. J. C **30**, 447 (2003)
60. DELPHI Collaboration, P. Abreu et al., Phys. Lett. B **511**, 159 (2001)
61. The LEP Collaborations ALEPH, DELPHI, L3 and OPAL, and the LEP W Working Group, Combined Preliminary Results on the Mass and Width of the W Boson Measured by the LEP Experiments, note LEPEWWG/MASS/2001-02, ALEPH 2001-044 PHYSIC 2001-017, DELPHI 2001-122 PHYS 899, L3 Note 2695, OPAL TN-697, contribution to EPS 2001, available at http://delphiwww.cern.ch/pubxx/delnote/public/2001_122_phys_899.ps.gz
62. DELPHI Collaboration, J. Abdallah et al., Measurement of the mass and width of the W boson in e^+e^- collisions at $\sqrt{s} = 161$–209 GeV, paper in preparation
63. N. Kjaer, M. Mulders, Mixed Lorentz boosted Z^0's, CERN-OPEN-2001-026
64. L3 Collaboration, P. Achard et al., Phys. Lett. B **561**, 202 (2003)
65. OPAL Collaboration, G. Abbiendi et al., Eur. Phys. J. C **45**, 291 (2006)
66. OPAL Collaboration, G. Abbiendi et al., Eur. Phys. J. C **45**, 307 (2006)
67. ALEPH Collaboration, S. Schael et al., Eur. Phys. J. C **47**, 309 (2006)